Short-Time Water Caging and Elementary Prehydration Redox Reactions in Ionic Environments

Y. Gauduel,* A. Hallou, and B. Charles

Laboratoire d'Optique Appliquée, CNRS UMR 7639 and INSERM U451, Ecole Polytechnique−ENS Techniques Avancées, 91761 Palaiseau Cedex, France

Received: July 29, 2002; In Final Form: November 22, 2002

This article deals with the direct probing of water cages that assist two well-defined prehydration electron transfers (PHETs) with the reactive metal cation Cd^{2+}. Early electron photodetachment processes are triggered by a two-photon UV excitation of aqueous halide ion Cl^- ($R = [H_2O]/[CdCl_2] = 110$). Concomitant with an ultrafast Cd^{2+} reduction by IR p-like excited electron (*J. Phys. Chem. A* **1998**, *102*, 7795), a subpicosecond oxidoreduction reaction occurs in caged three-body complexes $\{Cl\bullet\bullet e^-\bullet\bullet Cd^{2+}\}_{aq}$. Near-IR spectroscopic measurements give a PHET frequency of $1.38 \pm 0.02\ 10^{12}\ s^{-1}$. This reduction reaction is 70 times faster than a diffusion-controlled bimolecular reaction between aqueous Cd^{2+} ions and fully hydrated electrons (s-state). Femtosecond spectroscopic data indicate that preexisting bridging water-molecule-bonded $Cl^-\cdots Cd^{2+}$ pairs (SSIP-like configurations) assist efficient prehydration electron transfer. Because the 4s-like orbital radius of nascent $\{Cl\bullet\bullet e^-\bullet\bullet Cd^{2+}\}_{aq}$ configurations is larger than the mean distance of $Cd^{2+}-Cl^-$ ion pairs in a first coordination sphere of Cd^{2+} ions (∼2.6 Å), it is suggested that an overlap between a 4s electron orbital and the localized Cd^{2+} orbital favors an early inner-sphere electron transfer. For the first time, a nonlinear relationship is defined between the rate of Cd^{2+} univalent reduction and the energy level of the trapped electron (IR e^-_p, $\{Cl\bullet\bullet e^-\bullet\bullet Cd^{2+}\}_{aq}$, e^-_{aq}). We conclude that the short-time water cagings govern the course of PHET events and influence early branchings between elementary oxidoreduction reactions in ionic environments.

1. Introduction

Time-dependent solute−solvent couplings that assist or impede charge-transfer processes are attracting growing experimental and theoretical interest for physical and biological chemistry.[1−10] In the framework of the well-known Marcus theory, the solvent responses that accommodate a sudden charge repartitioning between donors and acceptors affect the crossing zone of nonequilibrium electronic states and finally govern the rate of electron-transfer reactions.[1,11−14] Several parameters including the free energy gap, solvent reorganization energy, donor/acceptor electron matrix element, and time-dependent electronic polarizability of solvent molecules can influence the course of elementary electron-transfer reactions.[15−20] The nature of transient interactions between solvated donor and acceptor is particularly important when adiabatic or nonadiabatic charge-transfer processes take place in specific structures such as solvent-bridged ion pairs. Numerous spectroscopic investigations of transient ion or radical pairs and intracomplex geometrical rearrangements have raised the importance of dynamical solvent responses.[21−29] A complete understanding of the primary events that govern oxidoreduction reactions requires the real-time probing of transient intermediates. Interesting redox processes involve geminate cage back electron recombinations or ultrafast univalent reductions.

Some fundamental aspects of charge-transfer processes include the role of water molecules during an ultrafast relaxation of nonequilibrium electrons.[30−34] At early times, primary electron transfers can be dramatically complicated by the interplay that exists between solvation processes and ultrafast radical reactions. For instance, when excess electron density is centered on nascent prototropic entities such as the aqueous hydronium ion $(H_3O^+)_{nH_2O}$ or hydroxyl radical (OH), ultrafast cage back electron−radical pair recombinations compete with the subpicosecond electron hydration channel. Selective H/D isotopic effects raise the important contribution of concerted electron−proton transfers.[35]

Aqueous electrolyte solutions, for which different ion−ion pair correlation functions are defined by neutron or X-ray diffraction and computed simulations,[36−66] represent a paradigm for the investigation of time-dependent molecular solvent responses that assist charge repartitioning between small reactants. Pioneering experimental works devoted to the femtosecond investigation of electron photodetachment from aqueous ferrocyanide or halide ions[67−69] have paralleled the development of numerical simulations. These simulations include molecular dynamics (MD), quantum path integral Monte Carlo (QPIMC), splitting operator method (SOM), and density functional density (DFT)[70−78] approaches. In liquid water, despite the apparent simplicity of halide ions (Cl^-, I^-), these anions exhibit complex interactions with solvent molecules via charge-transfer-to-solvent states (CTTS states).[79−81] The ground CTTS state of aqueous halide ions is characterized by a strong UV absorption band.[82−86] Recent works emphasize that transient excited CTTS states play a crucial role in photoinduced electron transfers.[68,87−91]

Femtosecond spectroscopic investigations of aqueous chloride ions have shown that a two-photon UV excitation of this anion triggers different ultrafast electron-transfer pathways (Figure 1). The relaxation of infrared highly excited CTTS states (CTTS**)

* To whom correspondence should be addressed. Phone: +33(0) 1 69 31 97 26. Fax: +33(0) 1 69 31 99 96. E-mail: gauduel@enstay.ensta.fr.

10.1021/jp021745p CCC: $25.00
Published on Web 02/27/2003

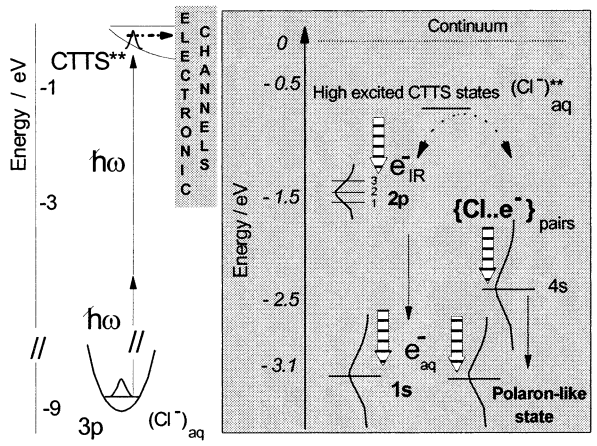

Figure 1. Energy level diagram of two well-characterized nonequilibrium electronic states [IR e^-_p, $(Cl\cdot\cdot e^-)_{pairs}$] and two fully relaxed configurations of an excess electron (s-like ground-state e^-_{aq} and polaron-like state) following a two-photon excitation (2×4 eV) of aqueous chloride ion with femtosecond UV pulses (representation adapted from Gauduel et al.[87]). The striped arrows indicate the electronic states investigated in the present study.

in less than 50 fs precedes the appearance of transient precursors of fully hydrated electrons: p-like excited electrons $(e^-_{IR})_{p\rightarrow s}$ and caged halogen−electron pairs $(Cl\cdot\cdot e^-)_{aq}$.[87] The direct probing of caged halogen−electron pairs $(Cl\cdot\cdot e^-)_{aq}$ with an optical multichannel analyzer gives a transient signature in the near-infrared region.[87b] Computed semiquantum molecular dynamics simulations of the $3p \rightarrow 4s$ transition of aqueous Cl^- suggest that a transient $(Cl\cdot\cdot e^-)_{aq}$ pair can be understood as an excess electron localized in the solvation shells of an aqueous chlorine atom.[77,91] From transient halogen−electron pairs, early branchings take place between efficient geminate cage back electron−chlorine atom recombination and complete adiabatic electron photodetachment. Experimentally, the ultrafast cage geminate recombination yields a halide ion in the highly excited vibrational state. This recombination process is strongly dependent on the chemical nature of the counterions (Na^+, Li^+, H^+).[87,92] In the presence of a nonreactive counterion, a fraction of caged halogen−electron pairs $\{Cl\cdot\cdot e^-\cdot\cdot X^+\}_{n H_2O}$ undergoes complete electron photodetachment and yields the adiabatic formation of polaron-like states $(X^+{:}e^-)_{aq}$. This second electron hydration channel is slower than that descended from a radiationless $p \rightarrow s$ transition of IR excited electron. Experimental H/D isotope substitution data raise the prevailing effect of water molecules on the behavior of near-infrared (nIR) caged three-body complexes $\{Cl\cdot\cdot e^-\cdot\cdot X^+\}_{n H_2O}$.[87c]

The femtochemistry of electrolyte aqueous solutions offers the opportunity to move forward some investigations of ultrafast elementary oxidoreduction reactions with charged reactants. The significant role of cations in early electron-transfer processes must be considered in the framework of ion-pair dynamics, ion−solvent correlation functions, short-range ordering of water molecules, solvent screening, and anisotropic electric field effects.[93−95] A first aspect of elementary oxidoreduction reactions in electrolyte solutions concerned the real-time probing of univalent reduction reactions by short-lived IR p-like excited electrons.[96,97] Cadmium ion was chosen for its excellent electron scavenger properties in the aqueous phase.[98] Magnesium ion was used as an unreactive cation because the consequence of ultrafast electron attachment is experimentally not apparent. Moreover, the excess electrons can be trapped in the vicinity of hydrated magnesium ions.[99]

A complete understanding of ultrafast prehydration oxidoreduction reactions requires that the short-time investigations of electron-transfer processes in solvent caged ion pairs be extended. The major concern of the present work is to elucidate whether a subpicosecond prehydration electron-transfer (PHET) reaction takes place in caged ion pairings (eq 1). We focus on the characterization of an ultrafast univalent reduction pathway inside the photoinduced three-body complex $\{Cl\cdot\cdot e^-\cdot\cdot Cd^{2+}\}_{aq}$.

$$(Cl^-\cdots Cd^{2+})_{aq} \xrightarrow{\text{photoexcitation}} \text{transient } \{Cl\cdot\cdot e^-\cdot\cdot Cd^{2+}\}_{aq} \xrightarrow{\text{PHET reaction}} (Cl\cdots Cd^+)_{aq} \quad (1)$$

This prehydration electron-transfer reaction is compared to other ultrafast electron-transfer channels and is discussed in terms of structural considerations. For the first time, we determine a relationship between the different trapping levels of an excess electron and the univalent reduction dynamics of aqueous metal cations. The direct probing of PHET events furthers the microscopic investigation of elementary redox reactions.

The paper is organized as follows: The experimental procedure is described in section 2. In section 3, we present experimental results, computed electron-transfer models for nonreactive and reactive cations, and the results of these models. Section 4 contains a general discussion of the discrimination of two subpicosecond univalent reduction pathways of aqueous cadmium ions. The paper ends with concluding remarks.

2. Experimental Section

Time-resolved spectroscopic experiments were performed with a pump−probe configuration. Femtosecond pulses centered at 620 nm were generated by a passively mode-locked CW dye ring laser. The colliding pulse mode-locked laser was followed by five amplifier stages. The compression of amplified beams through a four-prism arrangment allowed output pulses with energies above 1 mJ and typically with 70−90-fs durations at a 10−20 Hz repetition rate. The pump beam was generated by frequency doubling of amplified pulses in a 1-mm KDP crystal and focused on a quartz Suprasil cell. In the sample, the pump and probe beams overlapped by less than 0.5 mm. Photoinduced electron transfers were triggered by a two-photon excitation of aqueous halides ions (Cl^-) with femtosecond UV laser pulses (4 eV). The energy density of an excitation pulse at 310 nm was adjusted at $7 \pm 0.5\ 10^{10}$ W cm^{-2}, and the test beam was selected from a continuum generation with thin optical filters. The short-time dependence of photoinduced absorption signals were investigated with silicium (visible) and germanium (infrared) photodiodes. The different procedures used to define the position of zero delay time and instrumental response have been published elsewhere.[87]

Aqueous electrolyte solutions were prepared by dissolving $MgCl_2$ or $CdCl_2$ (purity = 99.999%) from Aldrich Chemical Co. in light water at a final concentration of 0.5 M. This concentration is defined by the molecular ratio R ($R = [H_2O]/[XCl_2]$, X = Mg, Cd). Under our experimental conditions, this parameter corresponds to an average number of 110 water molecules per solute molecule. Water was bidistilled in a quartz distillator with $KMnO_4$, and its resistivity was greater than 19 MΩ. Considering that the aqueous solute was fully dissociated ($XCl_2 \rightarrow 2Cl^- + X^{2+}$), the sharing of water molecules between three ionic entities satisfies the complete solvation shells of anion and cations. The electrolyte solutions exhibited an absorption

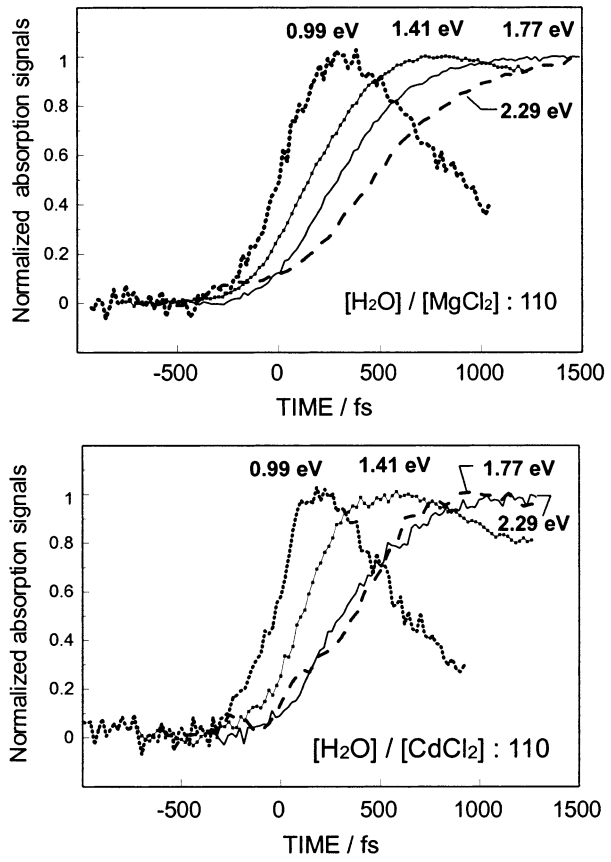

Figure 2. Short-time counterion effects (Mg^{2+} vs Cd^{2+}) on normalized absorption signals probed by femtosecond IR and visible spectroscopy following a two-photon excitation of aqueous chloride ions with femtosecond UV pulses (2 × 4 eV) at 294 K. The molecular ratio of aqueous electrolyte solutions equals 110 (R = H_2O/XCl_2; X = Mg, Cd).

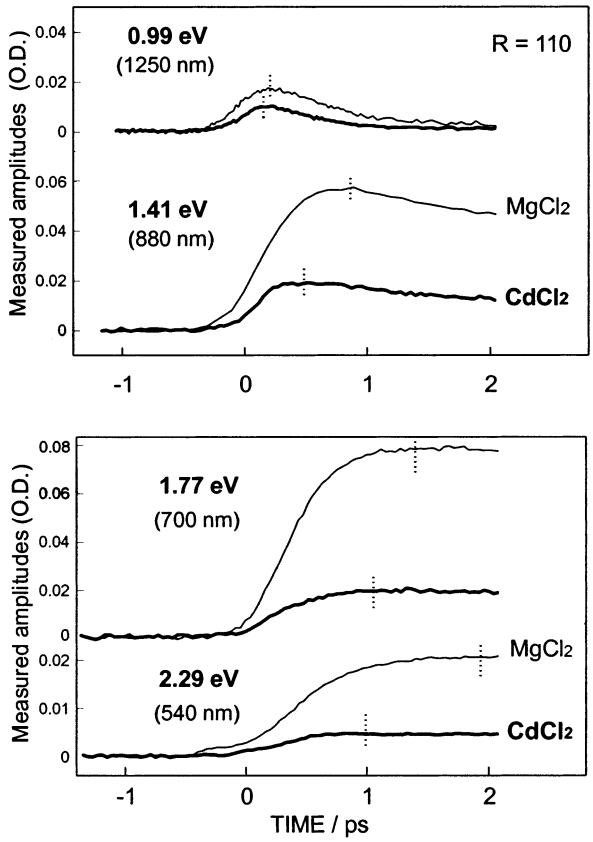

Figure 3. Short-time influence of a Mg^{2+}/Cd^{2+} ionic substitution on measured amplitudes of photoinduced IR and visible absorption signals in aqueous chloride solutions (H_2O/XCl_2 = 110; X = Mg, Cd).

of 0.01 at 310 nm. To avoid some undesirable oxidative processes or local heating of the electrolyte solutions, molecular oxygen was removed using a flow of pure nitrogen gas. Femtosecond spectroscopic experiments were performed at 294 K, using Suprasil cells continuously moved so that each amplified laser pulse excited a new region of the sample.

Femtosecond UV−IR spectroscopic data were analyzed with computed kinetic models developed on a Sun $C1^+$ Sparc workstation. These models take into account primary photophysical and photochemical events triggered by the two-photon excitation of aqueous chloride ions. The details of the computed kinetic models are given in the following section.

3. Results

3.A. Frequency Dependence of Signal Dynamics and Amplitude. The primary events triggered by femtosecond UV excitations of aqueous chloride ions (H_2O/XCl_2, X = Mg, Cd) were investigated by infrared and visible spectroscopy. A two-photon excitation of aqueous Cl^- (2 × 4 eV) induces very short-lived electronic states (highly excited charge-transfer-to-solvent states) and early electron photodetachment events. In the range 2.29−0.99 eV (540−1250 nm), the experimental curves exhibit a frequency dependence of amplitude and signal dynamics (Figures 2 and 3). After Mg^{2+} substitution by Cd^{2+}, the signal amplitude (S_{max}) decreases by 45% in the visible region (1.77 eV) and by 75% in the infrared region (0.99 eV). Additional information can be extracted from an analysis of the signal accumulation dynamics. This informatoion concerns the characteristic time $t_{S_{max}}$ for which the photoinduced absorption signals reach a maximum. In the spectral range 0.99−2.29 eV, the results of Figure 3 show that the substitution of Mg^{2+} by Cd^{2+} shortens the $t_{S_{max}}$ value. These time-resolved spectroscopic data were analyzed with computed kinetic models.

3.B. Details of Computed Kinetic Models. Figure 4 presents the details of computed kinetic models used for the characterization of photoinduced electron-transfer pathways in reference ($MgCl_2$) and reactive ($CdCl_2$) solutions. These models allow for an analysis of (i) the time dependence of reactive or unreactive channels in the nondiffusive and diffusive regimes and (ii) the frequency dependence of transient signal amplitudes.

3.B.1. Absorption Signal Dynamics. For each test wavelength (ω_T), the time-resolved absorption signal $S^{\omega_T}(\tau)$ triggered by an excitation beam (I_p) and probed by a test pulse (I_T) is expressed by the equation

$$S^{\omega_T}(t) = \sum_i [\alpha_i^{\omega_T} \int_{-\infty}^{+\infty} n_i(t-\tau) \mathrm{corr}^{\omega_P,\omega_T}(t)\, \mathrm{d}t] \qquad (2)$$

In this expression, the time-resolved analysis of absorption signals $S^{\omega_T}(t)$ includes the convolution between the excitation and test beams separated by a time delay of τ [$\mathrm{corr}^{\omega_T,\omega_P}(\tau)$] and the contributions of electronic populations n_i. The correlation function $\mathrm{corr}^{\omega_T,\omega_P}(\tau)$ represents an instrumental response that takes into account the temporal profiles of the pump and probe pulses and the overall broadening factors due to refractive index effects in liquid samples.[87] For a biphotonic process, this correlation function is defined as

$$\mathrm{corr}^{\omega_P,\omega_T}(t) = \int_{-\infty}^{+\infty} I_T(t+\tau)\, I_P^2(\tau)\, \mathrm{d}\tau \qquad (3)$$

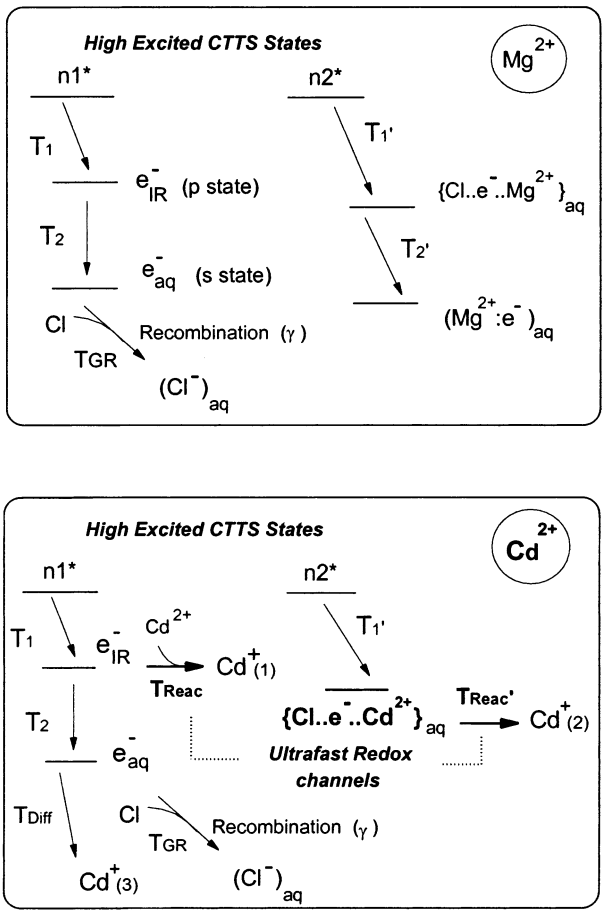

Figure 4. Synthetic representation of kinetic models developed for visible−IR spectroscopic investigations of ultrafast photoinduced electron transfers in $MgCl_2$ and $CdCl_2$ aqueous solutions. The models consider a two-photon excitation of aqueous halide ions, the formation of highly excited charge-transfer-to-solvent states (CTTS states**), and early electron photodetachment events. With Mg^{2+}, electronic channels yield two populations of fully hydrated electrons: e^-_{aq} and $(Mg^{2+}:e^-)_{aq}$. With the reactive Cd^{2+}, two prehydration electron-transfer reactions (PHET) are considered. For explanation, see the text.

At $\tau_{S_{max}}$, the calculated absorption signal ($S^{\omega_T}_{max}$) is maximum. This characteristic value is defined by the eq 4

$$S^{\omega_T}_{max} = \sum_i \alpha_i^{\omega_T} n_i^{\tau S_{max}} \tag{4}$$

In this expression, $\alpha_i^{\omega_T}$ is the absorption contribution of electronic state i at a given test wavelength (ω_T), and $n_i^{\tau S_{max}}$ represents the computed level of this transient electronic state at $\tau_{S_{max}}$. When the analysis is performed with experimental curves normalized between 0 and 1 [$S^{\omega_T}_{nor}(\tau)$], eq 4 becomes

$$S^{\omega_T}_{nor}(\tau) = \sum_i \alpha_i^{\omega_T} n_i(\tau) / \sum_i \alpha_i^{\omega_T} n_i(\tau_{S_{max}}) \tag{5}$$

where $n_i(\tau)$ represents the calculated level of transient state i at time delay τ. Computed fits of experimental signals probed at different wavelengths allow for the careful investigation of ultrafast electronic pathways.

3.B.2. Characterization of Transient Electronic Pathways. The kinetic models take into account the initial highly excited charge-transfer-to-solvent states (CTTS** states) triggered by femtosecond two-photon UV excitation of aqueous halide ion Cl^- (2 × 4 eV).

$$(Cl^-)_{aq} + 2h\nu \xrightarrow{t \ll 50\ fs} CTTS^{**} \xrightarrow{t \approx 50\ fs} \text{electron photodetachment} \tag{6}$$

The different electron photodetachment pathways reported in Figure 4 are expressed by eqs 7−12. A first channel concerns IR p-like excited electrons whose short-time behavior is investigated in aqueous $MgCl_2$ and $CdCl_2$ solutions.

$$\frac{dn_1^*}{dt} = \beta_P \frac{I_P^2(t)}{2h\omega_P} - \frac{n_1^*}{T_1} \tag{7}$$

In this expression, n_1^* represents the initial level of highly excited CTTS states of aqueous Cl^-, i.e., the precursors of IR prehydrated electrons $(e^-_{IR})_p$, and β_P is the absorption coefficient for the two-photon excitation of aqueous Cl^- ion. In $MgCl_2$ solution, the IR p-like excited electrons yield an electron hydration channel via a radiationless p → s transition. The time-dependent level of a p-like excited electron (e^-_{IR}) is expressed by

$$\frac{dn_{(e^-_{IR})}}{dt} = \frac{n_1^*}{T_1} - \frac{n_{(e^-_{IR})}}{T_2} \tag{8}$$

for which T_1 and T_2 are the trapping and solvation times, respectively.

In aqueous $CdCl_2$ solution, an ultrafast Cd^{2+} reduction by p-state excited electrons is considered (lower part of Figure 4). Previous femtosecond IR spectroscopic studies performed with ionic or molecular acceptors have shown that an early branching between reactive and nonreactive IR pathways cannot be ranked by a simple T_{Reac}/T_2 ratio. The major reason for this observation is the quantum character of p-like excited electrons during an ultrafast prehydration reduction.[96,97] Consequently, PHET with Cd^{2+} ions is characterized by a reaction probability, P_{Reac}, and a reaction time, T_{Reac}. A small fraction of IR p-like excited electrons follow a radiationless transition with a probability $P_{p\rightarrow s}$ and a hydration time T_2 (eq 9).

$$\frac{dn_{(e^-_{IR})}}{dt} = P_{Reac}\left(\frac{n_1^*}{T_1} - \frac{n_{(e^-_{IR})}}{T_{Reac}}\right) + P_{p\rightarrow s}\left(\frac{n_1^*}{T_1} - \frac{n_{(e^-_{IR})}}{T_2}\right) \tag{9}$$

Details on the short-time estimate of P_{Reac} and $P_{p\rightarrow s}$ have been presented and discussed in two recent papers.[96,97] For a given concentration of cadmium ions, the early partition between two ultrafast IR electronic pathways in terms of a probability ratio is determined from computed fits of IR signal dynamics and signal amplitudes.[96] The probability ratio $P_{Reac}/P_{p\rightarrow s}$ is calculated from the adjusted relative contributions of $e^-_{IR\ Reac}$ and $e^-_{IR\ p\rightarrow s}$.

From experimental and theoretical considerations of short-time electron delocalization in aqueous chloride solutions, our computed kinetic models consider a second electron photodetachment pathway (Figure 4). Considering the high polarizability of chlorine atoms, this channel involves a nascent $\{Cl\cdot\cdot e^-\cdot\cdot X^{2+}\}_{aq}$ complex formed via highly excited CTTS states (n_2^*). We have tested the hypothesis that a specific electron-transfer reaction triggered by the femtosecond UV excitation of caged ion pairings $\{Cl^-\cdots X^{2+}\}_{aq}$ involves short-lived three-body complexes $\{Cl\cdot\cdot e^-\cdot\cdot X^{2+}\}_{aq}$. Consequently, a Mg^{2+}/Cd^{2+} substitution would modify the behavior of transient complexes whose prevailing contribution peaks in the near-infrared region.

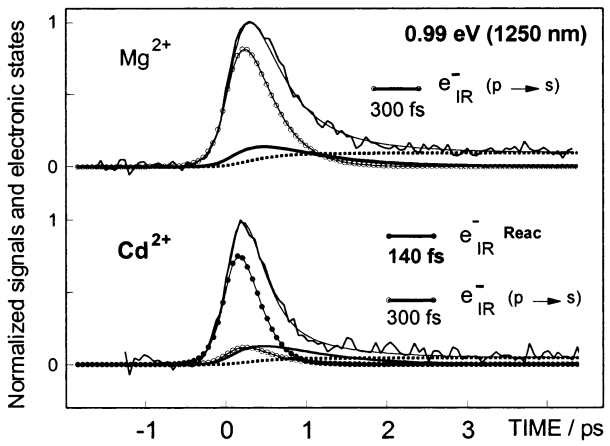

Figure 5. Computed IR analysis of electronic channels probed in reference ($MgCl_2$) and reactive ($CdCl_2$) aqueous solutions ($R = 110$). Smooth lines represent the best computed fits of nonexponential IR signal decays. The incomplete 0.99 eV signal recovery is ascribed to a low-energy tail contribution of the excess electron ground state (dotted line). In $MgCl_2$ solution, the IR dynamics is assigned to a nonadiabatic p → s transition of p-like excited electron (IR $e^-_{p\rightarrow s}$). In the presence of Cd^{2+} ions, the prevailing ultrafast univalent reduction by p-like excited electron ($e^-_{IR\ Reac}$) exhibits a time constant of 140 fs. The full line represents the small contribution of transient $\{Cl\cdot\cdot e^-\cdot\cdot X^{2+}\}_{aq}$ complexes.

For $MgCl_2$ solution, this electron photodetachment pathway is expressed by the two differential equations

$$\frac{dn_2^*}{dt} = \beta_P \frac{I_P^2(t)}{2h\omega_P} - \frac{n_2^*}{T_1'} \tag{10}$$

$$\frac{dn_{\{Cl\cdot\cdot e^-\cdot\cdot Mg^{2+}\}_{aq}}}{dt} = \frac{n_2^*}{T_1'} - \frac{n_{\{Cl\cdot\cdot e^-\cdot\cdot Mg^{2+}\}_{aq}}}{T_2'} \tag{11}$$

where n_2^* represents a second normalized population of CTTS** state, β_P is the absorption coefficient for a two-photon excitation of aqueous Cl^-, T_1' is the formation time of $\{Cl\cdot\cdot e^-\cdot\cdot Mg^{2+}\}_{aq}$, and T_2' is the cleavage dynamics of the complex.

In aqueous $CdCl_2$ solution, the early redox reaction involving a nascent three-body complex $\{Cl\cdot\cdot e^-\cdot\cdot Cd^{2+}\}_{aq}$ is defined as follows

$$\frac{dn_{\{Cl\cdot\cdot e^-\cdot\cdot Cd^{2+}\}_{aq}}}{dt} = \frac{n_2^*}{T_1'} - \frac{n_{\{Cl\cdot\cdot e^-\cdot\cdot Cd^{2+}\}_{aq}}}{T_{Reac}'} \tag{12}$$

In this equation, T_1' characterizes the accumulation dynamics of a three-body complex $\{Cl\cdot\cdot e^-\cdot\cdot X^{2+}\}_{aq}$, and T_{Reac}' is the dynamics of a second prehydration Cd^{2+} univalent reduction pathway.

3.C. Real-Time Probing of Prehydration Redox Reactions. *3.C.1. Prehydration IR Electron-Transfer Pathway.* Charge-transfer processes involving nonequilibrium electrons and fully relaxed states were investigated by infrared and visible spectroscopies. The main results are reported in Figures 5 and 6 and Tables 1 and 2. For aqueous $MgCl_2$ and $CdCl_2$ solutions, infrared signals exhibit noninstantaneous rise times. The best computed fits of IR signals illustrate the prevailing contribution of a direct electron photodetachment channel yielding p-state excited electrons $(e^-_{IR})_{p\rightarrow s}$. In a reference aqueous $MgCl_2$ solution, the accumulation time T_1 of $(e^-_{IR})_{p\rightarrow s}$ equals 130 ± 10 fs. This IR prehydration electron-transfer channel populates

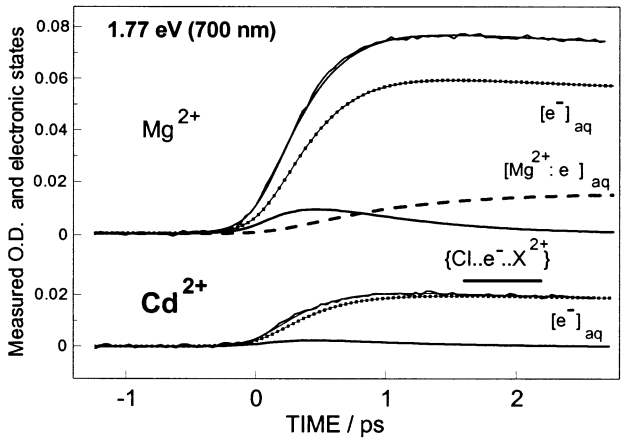

Figure 6. Influence of Mg^{2+}/Cd^{2+} substitution on the rise time and amplitude of absorption signals probed at 1.77 eV. The different contributions of electronic ground states are reported.

TABLE 1: Characteristic Times of Early Electron-Transfer Pathways in Chloride Aqueous Solution Containing Divalent Metal Cations[a]

solution parameters	nonreactive cation Mg^{2+}	reactive cation Cd^{2+}
IR p-like Excited Electron (IR e^-_p)		
T_1	130 ± 10 fs	130 ± 10 fs
T_2	300 ± 20 fs	300 ± 20 fs
T_{Reac}	−	140 ± 20 fs
$P_{p->s}$	1	0.1
P_{Reac}	0	0.9
nIR $\{Cl\cdot\cdot e^-\cdot\cdot X^{2+}\}_{aq}$ Complex		
T_1'	250 ± 10 fs	250 ± 10 fs
T_2'	750 ± 20 fs	
T_{Reac}'	−	720 ± 20 fs
Hydrated Electron Ground State (e^-_{aq})		
T_{Diff}	−	52 ± 1 ps
T_G	1.3 ± 0.1 ps	1.3 ± 0.1 ps
temporal ratio		
T_{Diff}/T_{Reac}'	−	70
T_{Diff}/T_{Reac}	−	370

[a] $H_2O/XCl_2 = 110$; X = Mg, Cd.

TABLE 2: Computed Spectral Contributions ($\alpha_i^{\omega T}$) of Different Electronic States to Visible−Infrared Absorption Signals Following the Femtosecond UV Excitation of Chloride Ions in Aqueous Electrolyte Solutions[a]

parameters	spectral contributions $(\alpha_i)^{\omega T}$ Mg^{2+}				spectral contributions $(\alpha_i)^{\omega T}$ Cd^{2+}			
states (eV)	0.99	1.41	1.77	2.29	0.99	1.41	1.77	2.29
IR $e^-_{p\rightarrow s}$	0.82	0.15	0.02	0	0.10	0.01	0.001	0
IR e^-_{Reac}	0	0	0	0	0.77	0.09	0.009	0
$\{Cl\cdot\cdot e^-\cdot\cdot X^{2+}\}_{aq}$	0.11	0.45	0.13	0.05	0.10	0.38	0.06	0.02
e^-_{aq}	0.06	0.31	0.59	0.60	0.03	0.52	0.93	0.98
$(X^{2+}:e^-)_{aq}$	0.01	0.09	0.26	0.35	0	0	0	0

[a] $H_2O/XCl_2 = 110$; X = Mg, Cd.

the fully hydrated electron state (s-state) via a radiationless p → s transition.

$$IR(e^-)_{p\rightarrow s} \xrightarrow[T_2 = 300\ fs]{\text{nonadiabatic p}\rightarrow\text{s transition}} (e^-_{aq}) \tag{13}$$

This transition follows an exponential decay with a time constant T_2 of 300 ± 20 fs. The prehydrated electron $(e^-_{IR})_{p\rightarrow s}$ represents about 80% of the transient signal probed at 0.99 eV. A low-energy tail of fully hydrated electrons (e^-_{aq}) contributes

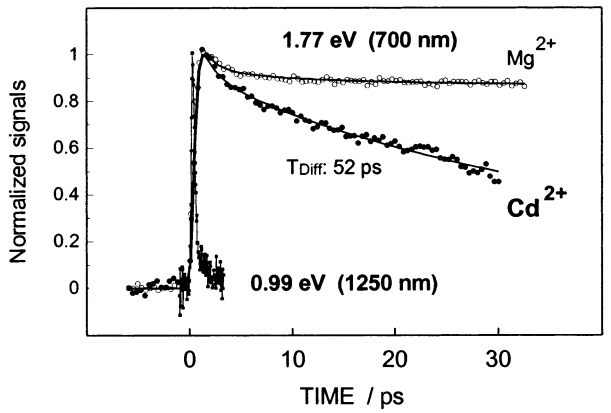

Figure 7. Comparison between ultrafast IR p-like electron transfer on cadmium ions (0.99 eV) and diffusion-controlled reaction with e^-_{aq} (1.77 eV). In reference $MgCl_2$ aqueous solution, the early visible signal decay is assigned to a 1D geminate recombination between a fraction of e^-_{aq} and chlorine atoms (eqs 15 and 16). In the presence of Cd^{2+}, the prevailing diffusion-controlled reaction ($e^-_{aq} + Cd^{2+} \rightarrow Cd^+$) follows a pseudo-first-order law with a time constant T_{Diff} of 52 ± 2 ps. The complex time dependence of e^-_{aq} is expressed by eq 18.

to the incomplete IR signal recovery (Figure 5). The correlation between the subpicosecond IR p → s transition and the electron hydration efficiency was investigated by visible spectroscopy of e^-_{aq}. Figure 6 reports the best computed fits of absorption signals probed at 1.72 eV. In aqueous $MgCl_2$ solution, e^-_{aq} is totally populated in less than 1.5 ps. An additional contribution ascribed to a long-lived electronic state (polaron-like state) is described in the following section.

The early consequences of the substitution of Mg^{2+} by reactive Cd^{2+} ions in the electron hydration channels are reported in Figures 5 and 6 and Tables 1 and 2. Femtosecond data for $CdCl_2$ solution show that the IR electron transfer is significantly influenced by aqueous Cd^{2+} ions. The transient IR absorption signal probed at 0.99 eV is fitted with a linear combination of short-lived electronic states. A prevailing contribution of the transient absorption signal (∼77%) is assigned to the ultrafast reduction of Cd^{2+} ion by IR p-like excited electrons $(e^-_{IR})_{Reac}$. This prehydration redox reaction is characterized by a pseudo-first-order time constant T_{Reac} of 140 ± 20 fs (eq 14).

$$(Cd^{2+})_{aq} + (e^-_{IR})_{Reac} \xrightarrow{T_{Reac} = 140\ fs} (Cd^+)_{aq} \qquad (14)$$

Femtosecond IR investigations show that an early branching takes place between two prehydration electron trajectories (IR $e^-_{p\rightarrow s}$ and IR e^-_{Reac}). Contrary to the femtosecond spectroscopic data obtained with $MgCl_2$ solution, the nonradiative p → s transition occurring in aqueous $CdCl_2$ solution represents a minor contribution (Figure 5, Table 2). Consequently, the early yield of fully hydrated electrons (e^-_{aq}) is significantly reduced by reactive Cd^{2+} ions (Figure 6).

At this stage of the analysis, we emphasize that the substitution of Mg^{2+} by Cd^{2+} also influences the picosecond fate of e^-_{aq} (Figure 7). In $MgCl_2$ solution, a fraction of this s-state exhibits an early geminate recombination with chlorine atom (eq 15).

$$(e^-_{aq}) + (Cl^\circ)_{aq} \xrightarrow{T_G} (Cl^-)_{aq} \qquad (15)$$

As previously shown with aqueous NaCl and LiCl solutions, the early recombination of e^-_{aq} with a Cl parent atom follows a diffusive 1D walk whose analytical solution is

$$[e^-_{aq}](t) = \int_{-\infty}^{+\infty} \frac{dn_{(e^-)_{aq}}(t)}{dt} \left[1 - \gamma + \gamma\ \mathrm{erf}\left(\frac{T_G}{t - t'}\right)^{1/2}\right] dt' \qquad (16)$$

with $n_{(e^-)_{aq}}(t) = N^\circ_{(e^-)_{aq}}\{1 - 1/(T_1 - T_2)[T_2 \exp(-t/T_2) - T_1 \exp(-t/T_1)]\}$. In eq 16, the nonexponential geminate recombination between e^-_{aq} and Cl atoms follows an asymptotic time dependence $1/\sqrt{t}$ of the signal decay.[87] The analytical solution contains two adjustable parameters: a 1D geminate recombination time T_G and a recombination probability γ. For $MgCl_2$ solution, the initial signal decay takes place within the first 5 ps after energy deposition. The best fits of experimental curves give $T_G = 1.3 \pm 0.1$ ps and $\gamma = 0.38 \pm 0.2$ (Figure 7).

In reactive $CdCl_2$ solution, a small fraction of e^-_{aq} follows the same nonexponential law (eq 16) and the adjustable parameters are similar to those obtained for $MgCl_2$ ($T_G = 1.3 \pm 0.1$ ps and $\gamma = 0.38$). These results emphasize that reactive Cd^{2+} metal cations do not totally prevent the early 1D geminate recombination of equilibrated hydrated electrons with coordinated chlorine parents. In the presence of Cd^{2+} ions, the prevailing part of e^-_{aq} follows pseudo-first-order dynamics with a time constant of T_{Diff}. This picosecond process is ascribed to a bimolecular diffusion-controlled reaction (eq 17).

$$(e^-_{aq}) + (Cd^{2+})_{aq} \xrightarrow{T_{Diff}} (Cd^+)_{aq} \qquad (17)$$

From the kinetic model detailed in the lower part of Figure 4, the complex fate of e^-_{aq} is expressed as

$$[e^-_{aq}](t) = \int_{-\infty}^{+\infty} \frac{dn_{e^-_{aq}}(t)}{dt} \left[\gamma\ \mathrm{erf}\left(\frac{T_G}{t - t'}\right)^{1/2}\right] dt' + \int_{-\infty}^{+\infty} \frac{dn_{e^-_{aq}}(t)}{dt} \left[(1 - \gamma) \exp\left(\frac{t - t'}{T_{Diff}}\right)\right] dt' \qquad (18)$$

The best computed fits give $T_{Diff} = 52 \pm 2$ ps (Figure 7). For our experimental conditions ($[H_2O]/[CdCl_2] = 110$), the calculated bimolecular reaction rate $k_{(e^-_{aq}) + (Cd^{2+})_{aq}}$ equals $3.8 \pm 0.1 \times 10^{10}\ M^{-1}\ s^{-1}$. This estimate agrees with available data in the literature.[98] We conclude that the diffusion-controlled reaction between Cd^{2+} and e^-_{aq} is ∼4×10^2 times slower than the prehydration reduction of Cd^{2+} ions by IR p-like excited electron $(e^-_{IR})_{Reac}$.

3.C.2. Subpicosecond ET in Caged Electron−Ion Pairs. A second ultrafast electron transfer was investigated by near-infrared spectroscopy. For that purpose, we analyzed the consequences of a Mg^{2+}/Cd^{2+} substitution on the behavior of transient three-body complexes $\{Cl\cdot\cdot e^-\cdot\cdot X^{2+}\}_{aq}$. The main results are summarized in Figures 8−10. In reference $MgCl_2$ solution, time-resolved data were fitted with a linear combination of different electronic contributions

$$S^{\omega_T}(t) = \alpha_1^{\omega_T}[e^-_{IR}](t) + \alpha_2^{\omega_T}[Cl\cdot\cdot e^-\cdot\cdot Mg^{2+}]_{aq}(t) + \alpha_3^{\omega_T}[e^-_{aq}](t) + \alpha_4^{\omega_T}[Mg^{2+}{:}e^-_{aq}](t) \qquad (19)$$

The adjusted parameters $\alpha_2^{\omega_T}$, $\alpha_3^{\omega_T}$, and $\alpha_4^{\omega_T}$ are the contributions of a nascent $\{Cl\cdot\cdot e^-\cdot\cdot Mg^{2+}\}_{aq}$ complex and electron ground states $[e^-_{aq}, (Mg^{2+}{:}e^-)_{aq}]$, respectively. The best computed fits of near-infrared signals give a significant contribution of transient $\{Cl\cdot\cdot e^-\cdot\cdot Mg^{2+}\}_{aq}$ complex, whose

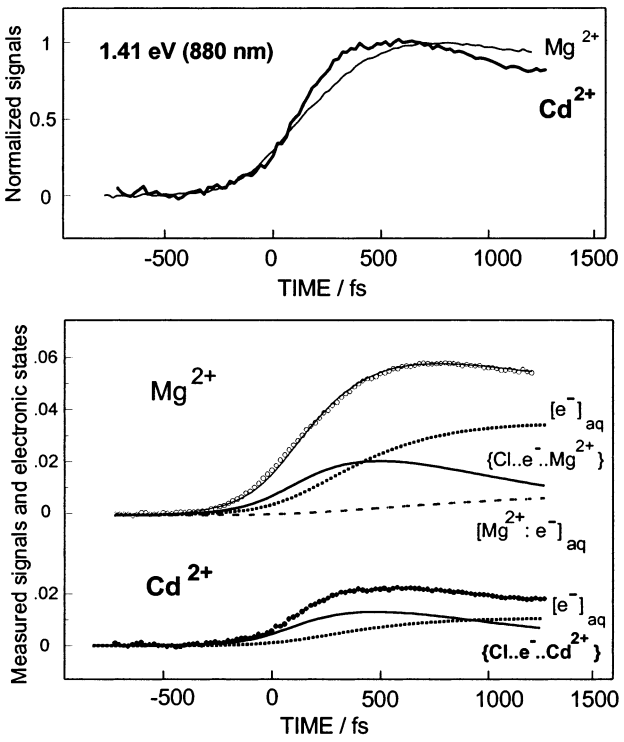

Figure 8. Near-IR probing of electronic dynamics following the femtosecond UV excitation of aqueous $MgCl_2$ and $CdCl_2$ solutions (R = 110). (Upper) details of normalized signal rise times at 1.41 eV. The smooth lines represent the best computed fits of experimental data. (Lower) effect of Mg^{2+}/Cd^{2+} substitution on measured signal amplitudes and computed levels of electronic states of the nascent $\{Cl\cdot\cdot e^{-}\cdot\cdot X^{2+}\}_{aq}$ complex. The minor contribution of p-like excited electrons is not reported. For explanation, see the text.

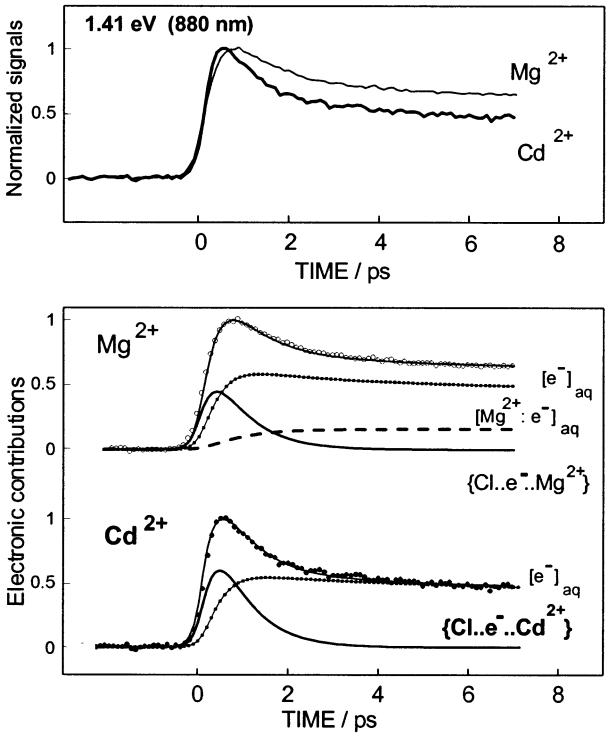

Figure 9. Picosecond effects of cadmium ions on transient electronic states probed at 1.41 eV. In reference aqueous $MgCl_2$ solution ($H_2O/MgCl_2$ = 110), a transient $\{Cl\cdot\cdot e^{-}\cdot\cdot Mg^{2+}\}_{aq}$ complex contributes to the subpicosecond signal decay. The incomplete signal recovery is due to e^{-}_{aq} and polaron-like state $(Mg^{2+}:e^{-})_{aq}$. In the presence of reactive Cd^{2+} ions, an efficient reduction reaction from transient $\{Cl\cdot\cdot e^{-}\cdot\cdot Cd^{2+}\}_{aq}$ exhibits a time constant of 720 ± 30 fs. This PHET prevents the formation of a polaron-like state. The minor contribution of IR p-like excited electron is not reported.

subpicosecond relaxation yields a second electron hydration channel (eq 20).

$$\{Cl\cdot\cdot e^{-}\cdot\cdot Mg^{2+}\}_{aq} \xrightarrow{T_2'} (Mg^{2+}{:}e^{-})_{aq} + (Cl)_{aq} \qquad (20)$$

In this equation, the time dependence of the nIR $\{Cl\cdot\cdot e^{-}\cdot\cdot Mg^{2+}\}_{aq}$ complex is defined by

$$\{Cl\cdot\cdot e^{-}\cdot\cdot Mg^{2+}\}_{aq}(t) = N^{\circ}_{\{Cl\cdot\cdot e^{-}\cdot\cdot Mg^{2+}\}_{aq}}[T_2'/(T_2' - T_1')][T_2' \exp(-t/T_2') - T_1' \exp(-t/T_1')] \quad (21)$$

where T_1' and T_2' are the formation and relaxation times, respectively, of transient $\{Cl\cdot\cdot e^{-}\cdot\cdot Mg^{2+}\}_{aq}$.

For different temporal windows (2 and 10 ps), the best computed fits give T_1' = 250 ± 20 fs and T_2' = 750 ± 30 fs (Figures 8 and 9). At 1.41 eV, the contribution of transient $\{Cl\cdot\cdot e^{-}\cdot\cdot Mg^{2+}\}_{aq}$ represents 45% of the total signal. By scanning $MgCl_2$ aqueous samples with different probe wavelengths, a frequency dependence of the transient $\{Cl\cdot\cdot e^{-}\cdot\cdot Mg^{2+}\}_{aq}$ contribution was determined (Figure 10). The computed band centered around 1.41 eV is very similar to near-IR signatures of caged halogen−electron pairs probed by an optical multichannel analyzer equipped with a liquid-nitrogen-cooled CCD detector (Princeton Instruments) or determined from time-dependent spectral measurements.[87b,d] In these experiments, the direct observation of a near-infrared hump peaking around 1.4 eV is totaly independent of a computed kinetic model.

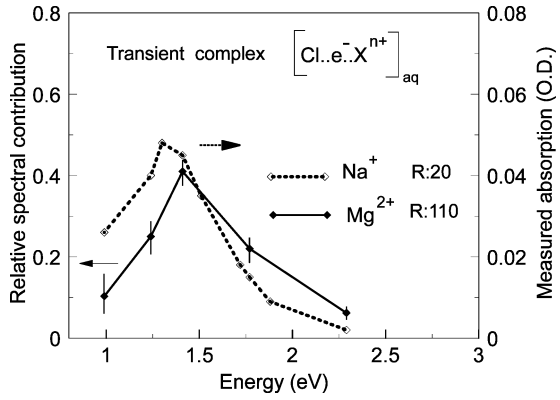

Figure 10. Computed spectral contribution of the transient $\{Cl\cdot\cdot e^{-}\cdot\cdot Mg^{2+}\}_{aq}$ complex following two-photon excitation of an aqueous $MgCl_2$ solution with femtosecond UV pulses (2 × 4 eV). The calculated spectral data are extracted from the kinetic data reported in Figure 4. By comparison, the measured nIR spectrum of the nascent $\{Cl\cdot\cdot e^{-}\cdot\cdot Na^{+}\}_{aq}$ complex following femtosecond excitation of NaCl aqueous solution is reported (data adapted from Gauduel et al.[87b]).

The fully relaxed electrons contribute to an incomplete nIR signal recovery. These ground states exhibit spectral signatures in the visible region (Figure 11). Spectroscopic investigations performed at 1.72 and 2.29 eV indicate the contribution of two well-defined electron ground states: s-like hydrated electrons (e^{-}_{aq}) and a polaron-like state $[(Mg^{2+}:e^{-})_{aq}]$ originating in a radiationless p → s transition and an adiabatic $\{Cl\cdot\cdot e^{-}\cdot\cdot Mg^{2+}\}_{aq}$ relaxation, respectively (eqs 13 and 20). The first electron hydration channel yielding e^{-}_{aq} is largely populated in less than

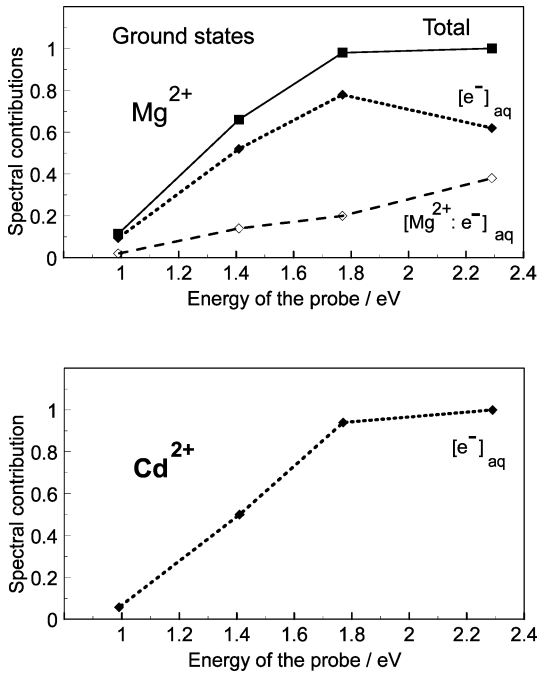

Figure 11. Relative spectral contribution of electron ground states following the femtosecond UV excitation of chloride ion in aqueous $MgCl_2$ and $CdCl_2$ solutions ($R = H_2O/XCl_2 = 110$). In aqueous $MgCl_2$ solution, e^-_{aq} and the polaron-like state $(Mg^{2+}:e^-)_{aq}$ contribute to a nonhomogeneous distribution of electron ground states. Inversely, a homogeneous population of e^-_{aq} is observed in $CdCl_2$ solution.

1 ps. The second electron hydration channel takes place in 3 ps (Figures 6, 12, and 13). The time dependence of the polaron-like state $(Mg^{2+}:e^-)_{aq}$ is expressed by the following equation

$$(Mg^{2+}:e^-)_{aq}(t) = N^{\circ\prime}_{(Mg^{2+}:e^-)_{aq}}\{1 - 1/(T_1' - T_2')[T_2' \exp(-t/T_2') - T_1' \exp(-t/T_1')]\} \quad (22)$$

The frequency dependence of the overall signal rise time along the high-energy tail of fully relaxed electrons depends on the relative spectral contributions of e^-_{aq} and $(Mg^{2+}:e^-)_{aq}$. At 2.29 eV, the residual component between the computed fit and experimental curve indicates that inhomogeneous solvent dynamics (ultrafast electronic response, librational motions, and/or slower solute−solvent frictional couplings) induce a time-dependent spectral shift. This spectral behavior is ascribed to dispersive responses of solvent molecules in the vicinity of nascent polaron-like state $(Mg^{2+}:e^-)_{aq}$. According to the polaron theory developed for ionic solutions,[100−102] the fraction of time spent by excess electrons in the aqueous environment of Mg^{2+} would increase the electron hydration energy and favor a slight blue shift of the nascent $(Mg^{2+}:e^-)_{aq}$.

The substitution of Mg^{2+} by Cd^{2+} significantly influences the course of elementary electron transfer in caged electron−ion pairs. These effects concern the amplitude and dynamics of photoinduced absorption signals (Figures 8 and 9). Near-IR absorption signals were analyzed with the computed kinetic model reported in the lower part of Figure 4. For different temporal windows (2 and 10 ps), we determined whether a prehydration reduction of Cd^{2+} takes place in the nascent $\{Cl\cdot\cdot e^-\cdot\cdot Cd^{2+}\}_{aq}$ complex (eq 23).

$$\{Cl\cdot\cdot e^-\cdot\cdot Cd^{2+}\}_{aq} \xrightarrow{T_{Reac}'} (Cd^+)_{aq} + (Cl)_{aq} \quad (23)$$

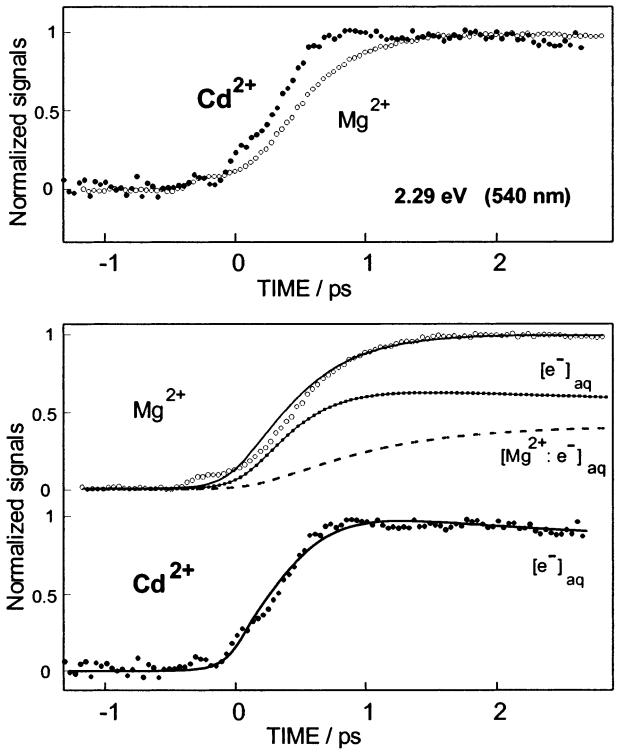

Figure 12. Short-time effects of Mg^{2+}/Cd^{2+} substitution on the absorption signal accumulation at 2.29 eV (upper) and the short-time contributions of fully relaxed electron (lower). In the presence of the reactive cation Cd^{2+}, the formation of the polaron-like state is completely hindered by a prehydration redox reaction in transient nIR $\{Cl\cdot\cdot e^-\cdot\cdot Cd^{2+}\}_{aq}$ complexes.

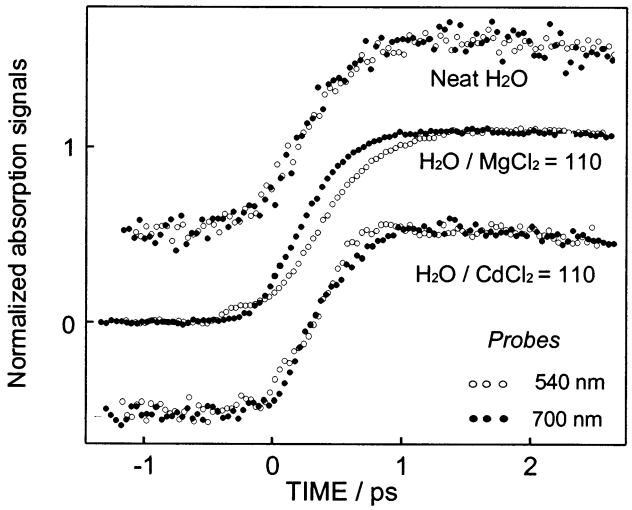

Figure 13. Comparative effects of water molecules and aqueous magnesium and cadmium ions on the electron hydration dynamics probed at 1.77 eV (700 nm) and 2.29 eV (540 nm). In pure water and aqueous $CdCl_2$ solution, the photoinduced signal rise time characterizes a homogeneous population of fully hydrated electrons e^-_{aq}. In $MgCl_2$ solution, the frequency dependence on the signal rise time is assigned to the dual contributions of e^-_{aq} and $(Mg^{2+}:e^-)_{aq}$.

At 1.41 eV, time-resolved spectroscopic data were fitted with a linear combination of contributions of short-lived nonequilibrium electronic states and fully relaxed electrons

$$S^{1.41}(t) = \alpha_{1a}^{\omega_T}(e^-_{IR\ p\rightarrow s})(t) + \alpha_{1b}^{\omega_T}(e^-_{IR\ Reac})(t) + \alpha_2^{\omega_T}\{Cl\cdot\cdot e^-\cdot\cdot Cd^{2+}\}_{aq}(\tau) + \alpha_3^{\omega_T}(e^-_{aq})(t) \quad (24)$$

In this expression, $\alpha_2^{\omega_T}$ is the contribution of nIR three-body

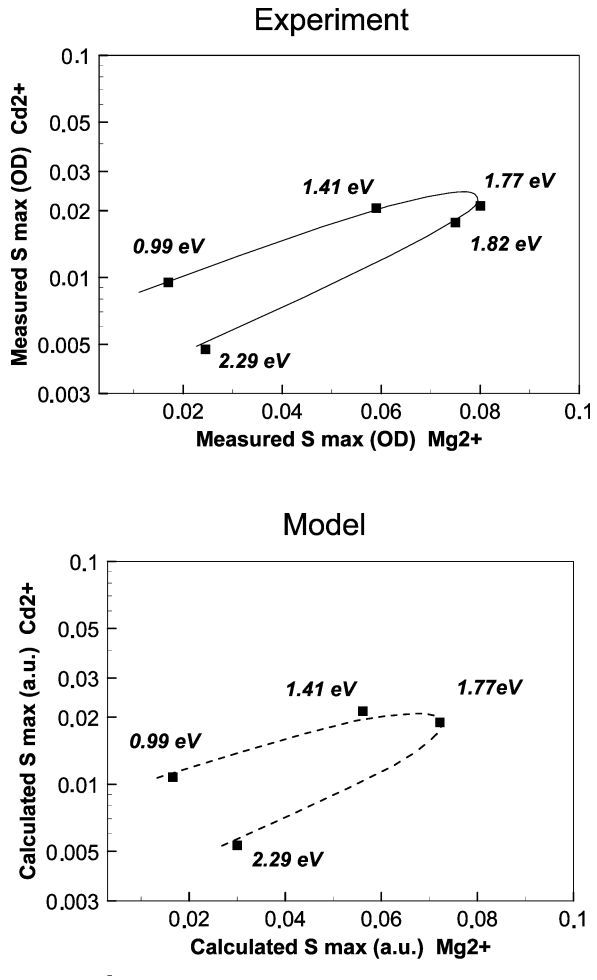

Figure 14. (A) Measured frequency dependence of the absorption signal amplitude (S_{max}) solutions following two-photon femtosecond UV excitation in aqueous $MgCl_2$ and $CdCl_2$. (B) Computed estimates of the frequency dependence of the signal amplitude using the kinetic models of Figure 4. The smooth lines are used as a guide for the eyes.

complex $\{Cl\cdot\cdot e^-\cdot\cdot Cd^{2+}\}_{aq}$. At 1.41 eV, $\alpha_2^{1.41}$ equals 0.38. The dynamics of this transient state is expressed by the equation

$$\{Cl\cdot\cdot e^-\cdot\cdot Cd^{2+}\}_{aq}(t) = N^\circ[T_{Reac}'/(T_{Reac}' - T_1')][T_{Reac}' \exp(-t/T_{Reac}') - T_1' \exp(-t/T_1')] \quad (25)$$

where T_1' is the $\{Cl\cdot\cdot e^-\cdot\cdot Cd^{2+}\}_{aq}$ formation time and T_{Reac}' is the dynamics of ultrafast Cd^{2+} reduction inside this transient complex. The best computed fits of nIR experimental curves give $T_1' = 250 \pm 20$ fs and $T_{Reac}' = 720 \pm 20$ fs (Figures 8 and 9 and Table 1). As reported in Table 2, the other terms of eq 24 represent the contributions of e^-_{aq} ($\alpha_3^{1.41} \approx 0.52$) and IR p-like excited electron ($\alpha_{1a}^{1.41} + \alpha_{1b}^{1.41} \approx 0.10$).

Contrary to spectroscopic data obtained with aqueous $MgCl_2$ solution, the relaxation of a $\{Cl\cdot\cdot e^-\cdot\cdot Cd^{2+}\}_{aq}$ complex does not yield polaron-like states. This important result has been completely investigated by visible spectroscopy. The main results are summarized in Figures 6 and 11−13 and Table 2. At 1.77 and 2.29 eV, the best computed fits give a prevailing contribution of e^-_{aq}. This electronic ground state is populated in less than 1.5 ps after UV energy deposition. A key point concerns the absence of a frequency dependence of visible signal rise times with $CdCl_2$ aqueous solution (Figure 13). This result indicates that the nascent e^-_{aq} population is homogeneous because the subpicosecond formation of the polaron-like state is totally hindered in the transient $\{Cl\cdot\cdot e^-\cdot\cdot Cd^{2+}\}_{aq}$ complex. A similar situation is observed in pure liquid water. In this case, the early electron−proton transfers involve short-lived $\{H_3O^+\cdot\cdot e^-\cdot\cdot OH\}_{aq}$ complexes and prevent the formation of polaron-like states.[30−33]

To validate the consistency of our computed analysis, the amplitudes of femtosecond IR, nIR, and visible signals $S^{\lambda}_{max}(t)$ were compared with computed estimates. The main results are reported in Figure 14. For each probe wavelength, the total contribution of photoinduced electronic states to the calculated $S^{\lambda}_{max}(t)$ is expressed by eq 3. In the spectral range 2.29−0.99 eV (540−1250 nm), good agreement is observed between measured values and computed estimates of $S^{\lambda}_{max}(t)$. The computed kinetic models well capture (i) the contributions of transient IR p-like excited electrons (IR e^-_{Reac}) and nIR $\{Cl\cdot\cdot e^-\cdot\cdot Cd^{2+}\}_{aq}$ in ultrafast Cd^{2+} reductions and (ii) the early consequences of PHET events on the levels of fully relaxed electrons (e^-_{aq} and polaron-like state).

3.D. Indirect Probing of a PHET Reaction from Excited CTTS States. The involvement of short-lived nonequilibrium electrons in PHET reactions has been estimated from the calculation of C_{37}.[98,103−106] This parameter represents the ability of aqueous Cd^{2+} ions to perform a prehydration redox reaction with the IR precursor of fully hydrated electrons (eq 15). C_{37} is expressed by the concentration of cadmium ions required to reduce the early level concentration of e^-_{aq} to 1/e = 37% of a reference value determined with the $MgCl_2$ solution. The short-time C_{37} value of Cd^{2+} has been previously determined by the direct probing of the IR p-like excited electron and the hydrated electron ground state.[96] Figure 15 reports a time dependence of C_{37} calculated from the contribution of e^-_{aq} determined at 1.41 and 1.77 eV (Figures 6 and 8). These data demonstrate that an ultrafast prehydration electron transfer decreases the early e^-_{aq} level. At this stage of the analysis, we tentatively determine whether an ultrafast PHET pathway from precursors of nascent $\{Cl\cdot\cdot e^-\cdot\cdot Cd^{2+}\}_{aq}$ influences the level of this transient state (eq 26).

$$\text{precursor (CTTS**)} \xrightarrow{T_1'} \{Cl^-\cdot\cdot e^-\cdot\cdot Cd^{2+}\}_{aq} \xrightarrow{T_{Reac}'} (Cd^+)_{aq}(2) + (Cl)_{aq} \quad (26)$$

$$\xrightarrow{\text{ultrafast PHET transfer?}} (Cd^+)_{aq}(2) + (Cl)_{aq}$$

For that purpose, a short-time C_{37}' value was determined from the subpicosecond contribution of $\{Cl\cdot\cdot e^-\cdot\cdot X^{2+}\}_{aq}$ probed at 1.41 eV. This parameter characterizes the ability of Cd^{2+} to initiate a prehydration electron transfer with very short-lived precursors of $\{Cl\cdot\cdot e^-\cdot\cdot X^{2+}\}_{aq}$. More precisely, C_{37}' represents a concentration of Cd^{2+} ions required to reduce the short-time level of transient $\{Cl\cdot\cdot e^-\cdot\cdot Cd^{2+}\}_{aq}$ to 1/e of a reference value determined with $MgCl_2$. The consequence of ultrafast prehydration electron transfer on the transient $\{Cl\cdot\cdot e^-\cdot\cdot Cd^{2+}\}_{aq}$ population is defined by the expression

$$\frac{S^{\omega_T}_{\{Cl\cdot\cdot e^-\cdot\cdot Cd^{2+}\}_{aq}}(\tau)}{S^{\omega_T}_{\{Cl\cdot\cdot e^-\cdot\cdot Mg^{2+}\}_{aq}}(\tau)} = \exp^{-[Cd^{2+}]/C_{37}'(t)}$$

$$\Rightarrow C_{37}'(t) = \frac{0.5}{\ln\left[\dfrac{S^{\omega_T}_{\{Cl\cdot\cdot e^-\cdot\cdot Mg^{2+}\}_{aq}}(\tau)}{S^{\omega_T}_{\{Cl\cdot\cdot e^-\cdot\cdot Cd^{2+}\}_{aq}}(\tau)}\right]} \quad (27)$$

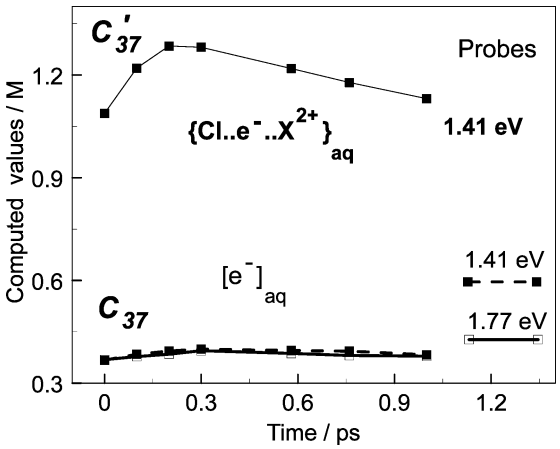

Figure 15. Short-time dependence of computed C_{37} and C_{37}' values of aqueous $CdCl_2$ solution ($R = 110$) during prehydration electron-transfer reactions. The time dependence of C_{37}' is determined from the direct probing of cage halogen−electron pairs $\{Cl\cdot\cdot e^{-}\cdot\cdot Cd^{2+}\}_{aq}$ at 1.41 eV. The C_{37} value is determined from the population of e^{-}_{aq} investigated at 1.41 and 1.77 eV. For explanations, see eqs 26 and 27.

In this equation, $S^{\omega_T}_{\{Cl\cdot\cdot e^{-}\cdot\cdot X^{2+}\}_{aq}}(\tau)$ represents the contribution of transient $\{Cl\cdot\cdot e^{-}\cdot\cdot X^{2+}\}_{aq}$ probed at 1.41 eV. The subpicosecond dependence of the computed C_{37}' value is reported in Figure 15. Within the first 300 fs, i.e., during the nIR signal rise time, the calculated C_{37}' value slightly increases. Beyond tS^{λ}_{max} (~500 fs at 1.41 eV), this C_{37}' value is 3 times higher than the C_{37} determined from hydrated electron ($C_{37}' = 1.15 \pm 0.1$ M, $C_{37} = 0.35 \pm 0.05$ M). These results suggest that an ultrafast PHET reaction involves the precursors of nIR three-body complex and strongly affects the level of $\{Cl\cdot\cdot e^{-}\cdot\cdot Cd^{2+}\}_{aq}$.

4. General Discussion

For the first time, a femtosecond spectroscopic study of two well-defined elementary univalent reductions of aqueous metal cations (Cd^{2+}) emphasizes that (i) two early electron transfers involve complex branchings between the IR p-like excited electron and the nIR three-body complex $\{Cl\cdot\cdot e^{-}\cdot\cdot X^{2+}\}_{aq}$ and (ii) an ultrafast Cd^{2+} reduction by p-like excited electron is more efficient than reduction from highly excited precursors of $\{Cl\cdot\cdot e^{-}\cdot\cdot X^{2+}\}_{aq}$.

In the presence of aqueous Cd^{2+} ions, our computed analyses of early ET reactions are focused on the time dependence of transient electronic levels. These analyses do not include a time-dependent spectral displacement of electronic bands. Because of the existence of two well-defined nonequilibrium electronic configurations, IR p-like excited electrons and $\{Cl\cdot\cdot e^{-}\cdot\cdot Cd^{2+}\}_{aq}$, it is difficult to extract simultaneously some information on the early electronic dynamics and time-dependent spectral moving. This technical point can be considered as follows. Previous studies devoted to the femtosecond radical chemistry of neat liquid water have clearly established that nonequilibrium configurations of hydrated electrons are dependent on short-lived prototropic radicals.[30,35] As a consequence, the 2D spectral envelope containing the contributions of short-lived IR and nIR nonequilibrium states ($e^{-}_{IR\ p\rightarrow s}$, $\{H_3O^{+}\cdot\cdot e^{-}\cdot\cdot OH\}_{aq}$) and nascent hydrated electrons (s-state) exhibits an apparent subpicosecond blue shift (see the Figure 4 of ref 35c). This time-dependent spectral behavior is more pronounced in deuterated water. Nevertheless, there is no significant frequency dependence of the signal rise time along the high-energy tail of e^{-}_{aq} (Figure 13). It has been shown that the short-time spectral behavior of excess electrons in pure liquid water is influenced by PHET reactions in transient nIR complexes $\{X_3O^{+}\cdot\cdot e^{-}\cdot\cdot OX\}_{aq}$ (X = H, D).[35c] This process introduces an untrue subpicosecond spectral blue shift between 1 and 1.7 eV but prevents a second electron hydration pathway. Consequently, a homogeneous e^{-}_{aq} population is observed in the visible region.

Concerning photoinduced electron transfers in aqueous $MgCl_2$ solution, the situation is different. The change in the signal rise time between 1.72 and 2.29 eV (Figure 13) is ascribed to a slight time-dependent spectral shift during the complete adiabatic electron detachment from the transient nIR complex $\{Cl\cdot\cdot e^{-}\cdot\cdot Mg^{2+}\}_{aq}$. We reasonably suggest that the nonhomogeneous solvent dynamics involving librational motions, solute−solvent frictional couplings, and/or Mg^{2+} anisotropic effects would influence the time-dependent spectral behavior during an electron relaxation in the vicinity of metal cations. However, up to now, we have no objective information permitting us to compute carefully a subpicosecond spectral moving of nIR bands with constant shapes in aqueous ionic environments. In the presence of reactive Cd^{2+} ions, the femtosceond spectroscopy of e^{-}_{aq} is very similar to previous results reported with pure liquid water. The absence of a frequency dependence on the signal rise time at 1.72 and 2.29 eV supports the conclusion that ground-state e^{-}_{aq} is populated from a radiationless p → s transition of IR excited electron. As shown in Figures 6, 9, and 11, the ultrafast PHET reaction inside nascent $\{Cl\cdot\cdot e^{-}\cdot\cdot Cd^{2+}\}_{aq}$ complexes does not contribute to a second solvation channel.

In the presence of Mg^{2+} and Cd^{2+} ions, the femtosecond spectroscopy of nonequilibrium electronic states triggered by a two-photon excitation of aqueous Cl^{-} ions allows for the direct investigation of solvent caging effects that assist elementary redox reactions at early times. We discuss at more length the salient features summarized in Figures 16−18.

4.A. Early ET Pathways in the Polarization Well of Aqueous Cl^{-}. The time-dependent responses of water molecules to a sudden change of charge repartioning of excited-state halide anion influence the primary steps of ultrafast PHET pathways. The first electronic configuration discriminated beyond 1.2 μm was ascribed to a high-lying excited state of aqueous halide ion (CTTS**) whose IR deactivation occurs in less than 50 fs.[87a] It is reasonable to consider that the short-lived highly excited CTTS** states participate in early electron photodetachment branchings.

In $MgCl_2$ aqueous solution, a direct photoinduced ET channel leads to p-like excited electrons (IR $e^{-}_{p\rightarrow s}$) whose coupling energy with surrounding water molecules is around −1.5 eV, i.e., ~0.5 eV below the liquid water conduction band. The subpicosecond p → s radiationless transition parallels a primary electron hydration channel whose ground-state e^{-}_{aq} is filled in less than 1.5 ps. In the presence of Cd^{2+} ions, an ultrafast redox reaction ($1/T_{Reac} = 7.1 \times 10^{12}$ s^{-1}) competes with a subpicosecond nonadiabatic p → s transition (Figure 16A). The computed data of Figure 17 predict that the byproduct $Cd^{+}_{(1)}$ appears before the e^{-}_{aq} population. Considering that semi-quantum MD simulations of nonequilibrium electron in water estimate that (i) the radius of gyration of p-like excited electrons equals 4 Å, (ii) the distance between the electronic center of mass and parent core can approach 16 Å,[71] we reasonably conclude that a femtosecond PHET pathway from IR p-like excited electrons involves some solvent-separated ion pairs (SSIP states) or quasi-free anion−cation configurations. We suggest that a through-bridge tunneling occurs from p-like excited electron trapping sites to quantum wells defined by aqueous Cd^{2+} ions.

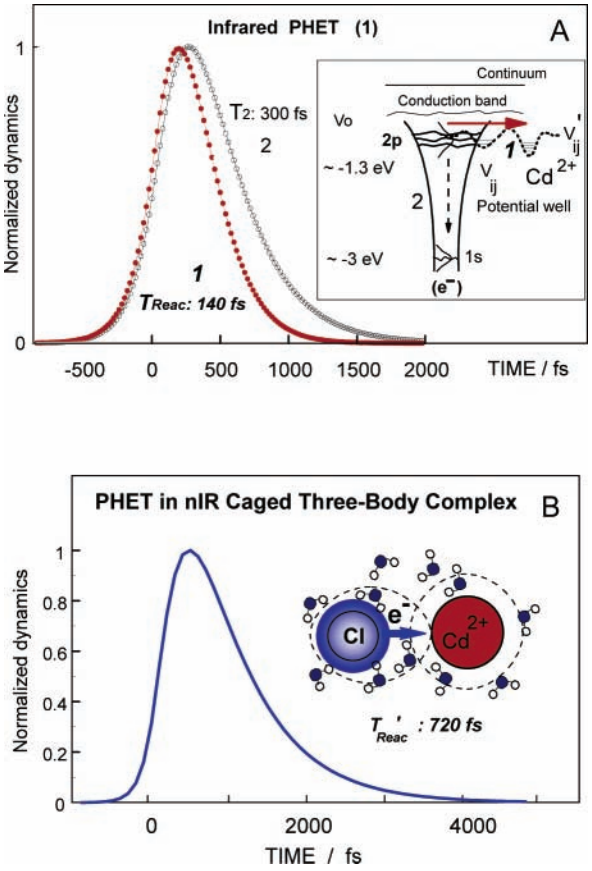

Figure 16. Comparative dynamics of two nonequilibrium electron-transfer channels triggered by a two-photon femtosecond UV excitation of aqueous electrolyte solution ($H_2O/XCl_2 = 110$; X = Mg, Cd). The upper part shows the difference between (1) an ultrafast prehydration reaction with Cd^{2+} and (2) a radiationless p → s transition undergoing electron hydration. The lower part depicts a prehydration redox reaction from a 4s electron orbital inside a nascent caged $\{Cl\cdot\cdot e^{-}\cdot\cdot Cd^{2+}\}_{aq}$ complex.

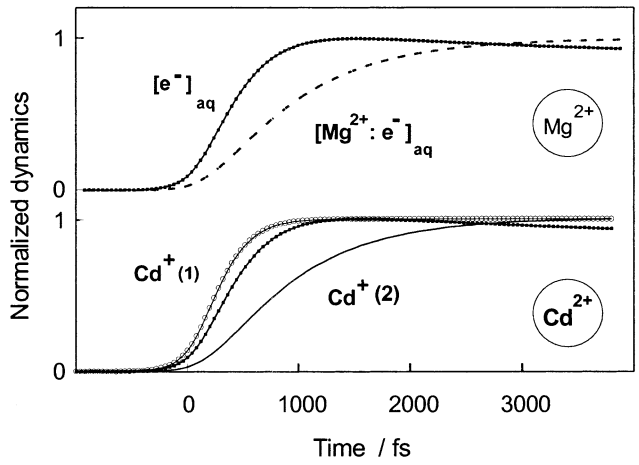

Figure 17. Computed analysis of accumulation dynamics of electronic ground states (byproducts) produced from electron trapping processes in aqueous environments (hydration channels) or prehydration redox reactions (PHETs) with Cd^2 ions.

Near-infrared investigations reported in Figures 8, 9, and 16B show that a second early electron-transfer pathway involves a nascent nIR $\{Cl\cdot\cdot e^{-}\cdot\cdot X^{2+}\}_{aq}$ complex, X = Mg, Cd. In the framework of a two-photon excitation of aqueous chloride ions, the short-lived $\{Cl\cdot\cdot e^{-}\cdot\cdot X^{2+}\}_{aq}$ complex is populated from highly excited CTTS states with a time constant T_1' of 250 fs. This process is 2 times slower than the appearance of IR p-like

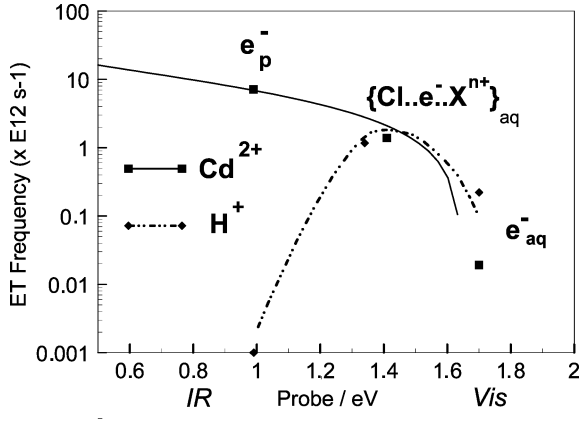

Figure 18. Nonlinear relationship between three levels of trapped electron probed by femtosecond IR and visible spectroscopies and the frequency of Cd^{2+} univalent reductions ($Cd^{2+} + e^- \rightarrow Cd^+$). The different electronic levels are the IR excited p-state electron, the nIR $\{Cl\cdot\cdot e^{-}\cdot\cdot Cd^{2+}\}_{aq}$ complex, and the ground s-state electron e^-_{aq}. The data on the electron reactions with hydrated H^+ are adapted from Gauduel et al.[92]

excited electrons ($T_1'/T_1 \approx 2.1$). Near-IR spectroscopic data permit one to establish that an electric field induced by Mg^{2+} favors an efficient electron photodetachment from the transient $\{Cl\cdot\cdot e^{-}\cdot\cdot Mg^{2+}\}_{aq}$ complex. This electron transfer yields polaron-like states $(Mg^{2+}:e^{-})_{aq}$ whose spectral signature peaks in the visible region. As reported in Figure 17, this nIR electronic pathway represents a delayed electron hydration channel.

Because the solvation energy of Mg^{2+} is higher than that of Cl^- [$U_{sol}(Mg^{2+}) \approx 1740$ kJ mol^{-1}, $U_{sol}(Cl^-) \approx 340$ kJ mol^{-1}),[60−62] subpicosecond electron transfer from transient $\{Cl\cdot\cdot e^{-}\cdot\cdot Mg^{2+}\}_{aq}$ complex can be assisted by water-bridged $Cl^-\cdots Mg^{2+}$ contacts. Monte Carlo studies of Mg^{2+} hydration have indicated that the ion and its first solvation shell can be understood as a supermolecule.[107] In this way, the metal ion can exert a long-range effect on the hydration shells of neighboring halide ions and induce a favorable spatial distribution of preexisting electron traps. Recent semiquantum MD simulations devoted to the very highly attractive potential of aqueous Mg^{2+} have established that excess electron density can be localized as well on the cation (spherical distribution) as in the region of a positive potential between Mg^{2+} and water molecules (nonnuclear traps).[99] According to polaron theory, these simulations emphasize that the total potential energy of localized electrons is determined by couplings with water molecules and cationic interactions.[100−102]

4.B. PHET Reaction in Caged Three-Body $\{Cl\cdot\cdot e^{-}\cdot\cdot Cd^{2+}\}_{aq}$ Complex. The most salient feature of the work is illustrated by Figure 16B. It concerns a subpicosecond PHET reaction from transient three-body $\{Cl\cdot\cdot e^{-}\cdot\cdot Cd^{2+}\}_{aq}$ complexes. Although the reduction reaction rate (T_{Reac}') is comparable to the nonreactive ET dynamics in $\{Cl\cdot\cdot e^{-}\cdot\cdot Mg^{2+}\}_{aq}$, the byproducts are different (eqs 20 and 23). With aqueous $CdCl_2$ solutions, the early electron transfer in caged $\{Cl\cdot\cdot e^{-}\cdot\cdot Cd^{2+}\}_{aq}$ yields Cd^+ ions whose UV signature peaks around 300 nm.[98b] The computed data reported in Figure 17 show that the second Cd^+ formation pathway [Cd^+ (2)] occurs after the electron hydration. This is explained by the fact that, in the nascent caged $\{Cl\cdot\cdot e^{-}\cdot\cdot Cd^{2+}\}_{aq}$ complex, the reaction rate $1/T_{Reac}'$ is 5 times lower than that of an IR p-like excited electron transfer on aqueous Cd^{2+} (Table 1).

Considering the good agreement that exists between femtosecond spectroscopic data of the electron photodetachment in aqueous chloride ion solutions[87] and semiquantum MD com-

putation of 4s-like excited aqueous chloride ions,[77,91] we reasonably assume that a neoformed nIR $\{Cl\cdot\cdot e^{-}\cdot\cdot Cd^{2+}\}_{aq}$ complex exhibits the 4s character of a caged electron−Cl atom pair. Following a 3p → 4s transition of 6.8 eV from the $(Cl^{-})_{H_2O}$ ground state whose hydration energy is around −9 eV, the energy level of nascent caged electron−halogen atom pairs is around −2.5 eV, i.e., ∼1 eV below the short-lived IR p-like excited electron.

The direct probing of a PHET reaction from short-lived $\{Cl\cdot\cdot e^{-}\cdot\cdot Cd^{2+}\}_{aq}$ complexes can be discussed in the framework of structural aspects of aqueous $CdCl_2$ solution and nonequilibrium electron dynamics. X-ray diffraction experiments on ion−ion pairs radial correlation functions argue for the presence of two chloride ions in the first coordination sphere of aqueous Cd^{2+} ions.[108] With a model including pseudo-octahedral complexes $[CdCl_2(H_2O)_4]$, it has been estimated that the mean distances of $Cd^{2+}-Cl^{-}$ and $Cd^{2+}-H_2O$ pairs are about 2.6 and 2.4 Å, respectively. Our femtosecond nIR spectroscopic data suggest that an ultrafast ET reaction from nIR $\{Cl\cdot\cdot e^{-}\cdot\cdot Cd^{2+}\}_{aq}$ configurations is assisted by preexisting solvent-bridged $Cd^{2+}-Cl^{-}$ complexations. From the work of Carminiti et al. on the structure of $Cd^{2+}\cdot\cdot Cl^{-}$ ion pairing in aqueous $CdCl_2$ solutions,[108] we conclude that the early univalent reduction of Cd^{2+} is likely dependent on water molecules shared with neighboring halide ions in the first coordination sphere of the divalent metal cations.

Semiquantum MD simulations with a polarized TIP4P water model predict that the polarizable character of chlorine atoms and the time-dependent polarizability of solvent molecules contribute to efficient electron confinement inside chlorine atom solvation shells.[91] For 4s-like chlorine−electron pairs, the estimated mean distance between the electronic center of mass and parent Cl core is about 6−7 Å. These computed MD simulations are compatible with our nIR spectroscopic data in the sense that nonstationary caged electron−Cl pairs exhibit a transient signature centered around 1.4 eV. Under our experimental conditions, the maximum of amplitude occurs at $tS^{\lambda}_{max} \approx 450$ fs (Figure 8). The extension of 4s-like electron−Cl atom pairs in liquid water satisfies the structural aspects of bridging solvent-molecule-bonded $Cl^{-}\cdot\cdot Cd^{2+}$ pairs. Because the radius of a 4s-like orbital inside the nascent $\{Cl\cdot\cdot e^{-}\cdot\cdot\cdot Cd^{2+}\}_{aq}$ configurations is larger than the mean distances between the $Cd^{2+}-Cl^{-}$ and $Cd^{2+}-H_2O$ pairs in the first coordination sphere of the Cd^{2+} ions (2.6 and 2.4 Å, respectively),[108] the overlap of a 4s electron wave function with the microenvironment of aqueous Cd^{2+} ions is favorable for ultrafast inner-shell electron transfer.

It is interesting to note that the exchange rate of water molecules in the first coordination sphere of Cd^{2+} ions (10^8 s^{-1}) is higher than for Mg^{2+} (10^6 s^{-1}).[109] For these positive counterions, water molecule exchange is several order of magnitude slower than (i) complete adiabatic electron photodetachment hydration from $\{Cl\cdot\cdot e^{-}\cdot\cdot Mg^{2+}\}_{aq}$ ($\nu_{2'} = 1/T_2' \approx 1.33$ 10^{12} s^{-1}) and (ii) the ultrafast PHET reaction inside the $\{Cl\cdot\cdot e^{-}\cdot\cdot Cd^{2+}\}_{aq}$ complex ($\nu_{Reac}' = 1/T_{Reac}' \approx 1.35$ 10^{12} s^{-1}). This subpicosecond redox process is 8 times faster than the mean residence time of water molecules in the first coordination layer of a chloride ion [$\tau_{H_2O}(Cl^{-}) \approx 5 \times 10^{-12}$ s].[110]

4.C. Electron Trapping Levels and Elementary Redox Reaction Dynamics. The results reported in Figure 18 show an interesting nonlinear relationship between electron trapping levels and univalent reduction dynamics. The univalent reduction of Cd^{2+} by a s-state hydrated electron (eq 17) follows a diffusion-controlled process whose pseudo-first-order dynamics is 70 times slower than that of a PHET reaction inside a 4s-like nIR $\{Cl\cdots e^{-}\cdots Cd^{2+}\}_{aq}$ complex and 4×10^2 times slower than an ultrafast reaction between IR p-like excited electron and Cd^{2+} ions (eq 14). These experimental results suggest the crucial role of water caging in the course of early redox events. In particular, the water bridge connecting electron donor Cl^{-} to acceptor Cd^{2+} (SSIP-like configurations) assists a prehydration electron-transfer reaction inside nascent three-body $\{Cl\cdot\cdot e^{-}\cdot\cdot Cd^{2+}\}_{aq}$ complexes.

Additional data reported in Figure 18 indicate that the nature of the cationic acceptor (Cd^{2+} vs H^{+}) influences the course of ultrafast PHET reactions. In preexisting caged $(Cl^{-}\cdots H^{+})_{aq}$ pairs, the nonlinear relationship observed between the electron trapping level and the elementary ET reaction dynamics exhibits a maximum for nIR $\{Cl\cdots e^{-}\cdots H^{+}\}_{aq}$ complex and a minimum for IR p-like excited electrons. Contrary to the results obtained with Cd^{2+}, a complex solvent caging effect is observed with H^{+}. The hydrated proton represents a specific electron acceptor for which the incomplete dissipation of excess electron kinetic energy by surrounding water molecules hinders the collapse of p-like electronic orbitals on dihydroniuiun ions ($H_5O_2^{+}$). As recently shown, the 4s character of a transient nIR $\{Cl\cdots e^{-}\cdots H^{+}\}_{aq}$ configuration is more favorable for efficient electron attachment on the dihydronium ion (hydrated proton) than a 2p-like IR prehydrated electron.[92] In the framework of a Marcus curve, the transient nIR $\{Cl\cdots e^{-}\cdots H^{+}\}_{aq}$ complex represents an optimized electronic configuration for fast electron transfer from aqueous halide ions to dihydronium acceptors ($H_5O_2^{+}$). This experimental result emphasizes that partial solvation of delocalized electrons is required to obtain an efficient electron−proton reaction.

An interesting point that emerges from the present study is that water caging and local polarization effects of chlorine atoms can be influenced by the chemical nature of the cations (Mg^{2+} vs Cd^{2+}). Because the kinetic energy dissipation of an excess electron by surrounding water molecules plays an essential role during the formation of electron-halide atom pairs,[77,91] the influence of the quantum polarization of water molecules must be contemplated. Experimental works on $\{Cl\cdot\cdot e^{-}\cdot\cdot Cd^{2+}\}_{aq}$ are in progress to determine whether anisotropic screening effects governed by water molecules assist a prehydrated electron transfer on Cd^{2+}. Considering recent calculations on specific couplings between chlorine atom and water molecules,[111] we should wonder whether nascent three-electron $2\sigma/1\sigma^{*}$ bonding between chlorine atom and water molecules participates in solvent reorganization during the subpicosecond univalent reduction of Cd^{2+}.

5. Concluding Remarks on PHET Reactions in Ionic Atmosphere

The direct investigation of PHET in aqueous ionic environments furthers our microscopic understanding of elementary redox reactions on early times.[97,112,113] The significant advance to be raised from our experimental work concerns femtosecond water caging effects during prehydration electron-transfer reactions in nascent $\{Cl\cdot\cdot e^{-}\cdot\cdot Cd^{2+}\}_{aq}$ configurations. Femtosecond spectroscopic investigations allow us to conclude that the relaxation of near-infrared electron−ion pairs $\{Cl\cdot\cdot e^{-}\cdot\cdot Cd^{2+}\}_{aq}$ parallels efficient nonequilibrium electron transfer on the cationic acceptor Cd^{2+}. This PHET pathway proceeds on roughly a 1-ps time scale.

The characterization of two ultrafast PHET pathways with aqueous Cd^{2+} ions would stimulate quantum MD simulations of elementary redox reactions in the prethermal regime ($t <$ 500 fs). In the framework of microscopic structures of caged

donor−acceptor configurations, computed quantum simulations would take into account the role of ion−ion correlation functions when a delocalized electron wave packet explores the fluctuating potential energy surface of a nonequilibrium three-body complex $\{Cl\cdot\cdot e^{-}\cdot\cdot Cd^{2+}\}_{aq}$. Experimental investigations of PHET reactions in the polarization CTTS well of aqueous halide ions provide guidance for further investigations of S_N1 reactions in a polarization caging regime;[114] the vibronic couplings that assist bond breaking/bond making in S_N2 reactions;[115] and, more generally, the electron-transfer events through fluctuating solvent bridges.

Acknowledgment. This work was supported by INSERM, the Chemical Department of CNRS, France (GdR 1017), and the Commission of the European Communities.

References and Notes

(1) Marcus, R. A. *J. Chem. Phys.* **1956**, *24*, 966. Sumi, H.; Marcus, R. A. *J. Chem. Phys*. **1985**, *84*, 4894. Marcus, R. A. *Rev. Mod. Phys.* **1993**, *65*, 599.

(2) Newton, M. D. *Chem. Rev*. **1991**, *91*, 767. Lami, A.; Santoro, F. *J. Chem. Phys.* **1997**, *106*, 94.

(3) Andrieux, C. P.; Gallardo, L.; Savéant, J. M.; Su, K. *J. Am. Chem. Soc*. **1996**, *108*, 638. Savéant, J. M. *J. Am. Chem. Soc.* **1992**, *114*, 10595. Bertran, J.; Gallardo, J. L.; Moreno, M.; Savéant, J. M. *J. Am. Chem. Soc*. **1996**, *118*, 5737.

(4) Mattay, J. *Angew. Chem., Int. Ed. Engl*. **1987**, *26*, 825.

(5) Moreau, M., Turq, P., Eds. *Chemical Reactivity in Liquids*; Plenum Press: New York, 1987.

(6) Gould, I. R.; Young, R. H.; Moody, R. E.; Farid, S. *J. Phys. Chem*. **1991**, *95*, 2068. Gould, I. R.; Farid, S. *J. Phys. Chem.* **1992**, *96*, 7635.

(7) Frantsuzov, P. A. *J. Chem. Phys.* **1999**, *111*, 2075. Frantsuzov, P. A.; Tachiya, M. *J. Chem. Phys.* **2000**, *112*, 4216.

(8) Yoshihara, Y.; Tominaga, K.; Nagasawa, Y. *Bull. Chem. Soc. Jpn.* **1995**, *68*, 696. Nagasawa, Y.; Yartsev, A. P.; Tominaga, K.; Bisht, P. B.; Johnson, A. E.; Yoshihara, K. *J. Phys. Chem.* **1995**, *99*, 653.

(9) Baskin, J. S.; Chachisvillis, M.; Gupta, M.; Zewail, A. H. *J. Phys. Chem. A* **1998**, *102*, 4158 and references therein.

(10) Jortner, J., Bixon, M., Eds. *Electron Transfer from Isolated Molecules to Biomolecules*; Advances in Chemical Physics Series; John Wiley & Sons: New York, 1999; Parts I and II, Vols. 106 and 107.

(11) Cukier, R. I. *J. Phys. Chem. A* **1999**, *103*, 5989. Skoutis, S. S.; Archontis, G.; Xie, Q. *J. Chem. Phys*. **2001**, *115*, 9444.

(12) Carter, E. A.; Hynes, J. T. *J. Chem. Phys.* **1991**, *94*, 5961.

(13) Asahi, T.; Mataga, N. *J. Phys. Chem*. **1989**, *93*, 6575. Mataga, N.; Nishikawa, N.; Asahi, T.; Okada, T. *J. Phys. Chem.* **1990**, *94*, 1443. Miyasaka, H.; Tabata, A.; Mataga, N. *J. Am. Chem. Soc.* **1993**, *115*, 7335.

(14) Kelley, A. M. *J. Phys. Chem. A* **1999**, *103*, 6891.

(15) Jortner, J.; Bixon, M. *J. Chem. Phys.* **1988**, *88*, 167. Rips, I.; Klafter, J.; Jortner, J. *J. Chem. Phys*. **1988**, *88*, 3246. Stell, G.; Zhou, Y. *J. Chem. Phys.* **1989**, *91*, 4869; **1989**, *91*, 4879; **1989**, *91*, 4885. Rips, I.; Pollack, E. *J. Chem. Phys*. **1995**, *103*, 7912. Rips, I. *Chem. Phys. Lett*. **1995**, *245*, 79. *J. Chim. Phys*. **1996**, *93*, 1591.

(16) Hynes, J. T. *Annu. Rev., Phys. Chem.* **1985**, *36*, 573. Hynes, J. T. *J. Stat. Phys.* **1986**, *42*, 149. Hynes, J. T. *J. Phys. Chem*. **1986**, *90*, 3701. Kim, H. J.; Hynes, J. T. *J. Phys. Chem.* **1990**, *94*, 2736. Keirstead, W. P.; Wilson, K. R.; Hynes, J. T. *J. Chem. Phys.* **1991**, *95*, 5256. Van der Zwan, G.; Hynes, J. T. *Chem. Phys.* **1991**, *152*, 169. 17.

(17) Burshtein, A. I.; Georgievski, Y. *J. Chem. Phys.* **1994**, *100*, 7319. 18.

(18) Gauduel, Y., Rossky, P. J., Eds.; *Ultrafast Reaction Dynamics and Solvent Effects*; AIP Press: New York, 1994; Vol. 298. Elementary Chemical Processes in Liquids and Solutions (Special Issue) *J. Chim. Phys.* **1996**, *93*, 1577−1938 and references therein.

(19) Maroncelli, M., Fleming, G. R. *J. Chem. Phys*. **1988** *89*, 875. Maroncelli M. *J. Chem. Phys.* **1991** *94*, 2084. Papazyan, A.; Maroncelli, M. *J. Chem. Phys.* **1993**, *98*, 6431. Horng, M. L.; Gardecki, J. A.; Papazyan, A.; Maroncelli, M. *J. Phys. Chem*. **1995**, *99*, 17311. *J. Chem. Phys*. **1995**, *102*, 2888. Grunwald, E.; Steel, C. *J. Am. Chem. Soc.* **1995**, *117*, 5687.

(20) Zewail, A. H. *J. Phys. Chem.* **1996**, *100*, 12701.

(21) Walker, G. C.; Aakesson, E.; Johnson, A. E.; Levinger, N. E.; Barbara, P. F. *J. Phys. Chem.* **1992**, *96*, 3728.

(22) *The Chemical Physics of Solvation*; Dogonadze, R. R., Kalman, E., Kornyshev, A. A., Ulstrup, J., Eds.; Studies in Physical and Theoretical Chemistry Series; Elsevier: New York, 1988; Vol. 38, Parts A−C. Bursulaya, B. D.; Zichi, D. A.; Kim, H. J. *J. Phys. Chem*. **1996**, *100*, 1392.

(23) Richert, R.; Wagner, H. *J. Phys. Chem*. **1995**, *99*, 10948.

(24) Gershgoren, E.; Banin, U.; Ruhman, S. *J. Phys. Chem. A* **1998**, *102*, 9. Chandra, A. *J. Chem. Phys. J.* **1999**, *110*, 1569.

(25) Tachiya, M.; Murata, S. *J. Phys. Chem.* **1992**, *96*, 8441; *J. Am. Chem. Soc.* **1994**, *116*, 2434.

(26) Stratt, R. M. *J. Chem. Phys.* **1994**, *100*, 6700.

(27) Lehr, L.; Zanni, M. T.; Frischkorn, C.; Weinkauf, R.; Neumark, D. M. *Science* **1999**, *284*, 635.

(28) Bagchi, B.; Biswas, R. *Adv. Chem. Phys.* **1999**, *109*, 207.

(29) Geissier, P. L.; Chandler, D. *J. Chem. Phys*. **2000**, *113*, 9759.

(30) Gauduel, Y.; Martin, J. L.; Migus, A.; Antonetti, A. Ultrafast Phenomena V; Fleming, G. R., Siegman, A. E., Eds.; Springer-Verlag: New York, 1986; p 308. Migus, A.; Gauduel, Y.; Martin, J. L.; Antonetti, A. *Phys. Rev. Lett*. **1987**, *108*, 318. Pommeret, S.; Antonetti, A.; Gauduel, Y. *J. Am. Chem. Soc.* **1991**, *113*, 9105.

(31) Long, F. H.; Lu, H.; Eisenthal, K. B. *Phys. Rev. Lett.*, **1990**, *64*, 1469. Shi, X.; Long, F. H.; Eisenthal, K. B. *J. Phys. Chem*. **1995**, *99*, 6917. Shi, X.; Long, F. H.; Lu, H.; Eisenthal, K. B. *J. Phys. Chem.* **1996**, *100*, 11903.

(32) Alfano, J. C.; Walhout, P. K.; Kimura, Y.; Barbara, P. F. *J. Chem. Phys*. **1993**, *98*, 5996. Kimura, Y.; Alfano, J. C.; Walhout, P. K.; Barbara, P. F. *J. Phys. Chem*. **1994**, *98*, 3450. Silva, C.; Walhout, P. K.; Yokoyama, K.; Barbara, P. F. *Phys. Rev. Lett.* **1998**, *80*, 1086. Yokoyama, K.; Silva, C.; Son, D. H.; Walhout, P. K.; Barbara, P. F. *J. Phys. Chem.* **1998**, *102*, 6957.

(33) Reuther, A.; Laubereau, A.; Nikogosyan, D. N. *J. Phys. Chem.* **1996**, *100*, 16794. Assel, A.; Laenen, R.; Laubereau, A. *J. Chem. Phys.* **1999**, *111*, 6869. Laenen, R.; Roth, T. *J. Mol. Struct.* **2001**, *37*, 598.

(34) Kummrow, A.; Emde, M. F.; Baltuska, A.; Pshenichnikov, M. S.; Wiersma, D. A. *J. Phys. Chem.* **1998**, *102*, 4172.

(35) (a) Gauduel, Y.; Pommeret, S.; Antonetti, A. *J. Phys. Chem*. **1993**, *97*, 134. (b) Gauduel, Y. In *Ultrafast Dynamics of Chemical Systems*; Simon, J. D., Ed.; Kluwer: Dordrecht, The Netherlands, 1994. (c) Gauduel, Y. In *Ultrafast Reaction Dynamics and Solvent Effects*; Gauduel, Y., Rossky, P. J., Eds.; AIP Press: New York, 1994; Vol. 298, p 191.

(36) Narten, A. H.; Vaslov, F.; Levy, H. A. *J. Chem. Phys.* **1973**, *58*, 5017. Triolo, R.; Narten, A. H. *J. Chem. Phys.* **1975**, *63*, 3624.

(37) Halle, B.; Karlström, G. *J. Chem. Soc., Faraday Trans. 2* **1983**, *79*, 1031; **1983**, *79*, 1047.

(38) Janoschek, R.; Weidemann, E. G.; Pfeiffer, H.; Zundel, G. *J. Am. Chem. Soc.* **1972**, *94*, 2387. Danninger, W.; Zundel, G. *J. Chem. Phys.* **1981**, *74*, 2769.

(39) Hertz, H. G.; Maurer, R. Z. *Phys. Chem. NF* **1983**, *135*, 107. Dippel, T.; Kreuer, K. D. *Solid State Ionics* **1991**, *46*, 3.

(40) Berkowitz, M.; Karim, O. A.; McCammon, J. A.; Rossky, P. J. *Chem. Phys. Lett*. **1984**, *105*, 577. Karim, O. A.; McCammon, A. *Chem. Phys. Lett.* **1986**, *132*, 219. Belch, A. C.; Berkowitz, M.; McCammon, J. A. *J. Am. Chem. Soc.* **1986**, *108*, 1755.

(41) Fornili, S. L.; M. Migliore, M.; Palazzo, M. A. *Chem. Phys. Lett.* **1986** *125*, 419.

(42) Ciccotti, G.; Ferrario, M.; Hynes, J. T.; Kapral, R. *J. Chem. Phys.* **1990**, *93*, 7137

(43) Rose, D. A.; Benjamin, I. *J. Chem. Phys.* **1991**, *95*, 6856.

(44) Zhu, S. B.; Robinson, G. W. *J. Chem. Phys.* **1992**, *95*, 4336.

(45) Walrafen, G. E.; Chu, Y. C. *J. Phys. Chem.* **1992**, *96*, 9127.

(46) Rey, R.; Guardia, E. *J. Phys. Chem.* **1992**, *96*, 4712. Rey, R.; Guardia, E.; Padro, J. A. *J. Chem. Phys.* **1992**, *97*, 1343.

(47) Chandrasekhar, J.; Spellmeyer, D. C.; Jorgensen, W. L. *J. Am. Chem. Soc.* **1984**, *106*, 903.

(48) Ohtaki, H.; Radnai, T. *Chem. Rev.* **1993**, *93*, 1157.

(49) Ohmine, I.; Tanaka, H. *Chem. Rev.* **1993**, *93*, 2545.

(50) Schuder, M.; Nesbitt, D. J. *J. Chem. Phys.* **1994**, *100*, 7250.

(51) Martin, C.; Lomba, E.; Lombardero, M.; Lado, F.; Hoye, J. S. *J. Chem. Phys.* **1994**, *100*, 1599.

(52) Laasonen, K.; Sprik, M.; Parrinello, M.; Car, R. *J. Chem. Phys.* **1993**, *99*, 9080. Tuckerman, M.; Laasonen, K.; Sprik, M.; Parrinello, M. *J. Chem. Phys.* **1995**, *103* 150; *J. Phys. Chem.* **1995**, *99*, 5749.

(53) Ando, K.; Hynes, J. T. *J. Mol. Liq.* **1995**, *64*, 25.

(54) Kowall, Y.; Foglia, F.; Helm, L.; Merbach, A. E. *J. Phys. Chem*. **1995**, *99*, 13078.

(55) Bhattacharya, I.; Voth, G. A. *J. Phys. Chem.* **1993**, *97*, 11253. Straub, J. B.; Calhoun, A.; Voth, G. A. *J. Chem. Phys.* **1995**, *102*, 529. Lobaugh, J.; Voth, G. A. *J. Chem. Phys.* **1996**, *104*, 2056. Paese, M.; Chawla, S.; Lu, D.; Lobaugh, J.; Voth, G. A. *J. Chem. Phys.* **1997**, *107*, 7428. Lobaugh, J.; Voth, G. A. *J. Chem. Phys*. **1996**, *104*, 2056. Pavese, M.; Chawla, S.; Lu, D.; Lobaugh, J.; Voth, G. A. *J. Chem. Phys.* **1997**, *107*, 7428.

(56) Blenzen, A.; Foglia, F.; Furet, E.; Helm, L.; Merbach, A. E.; Weber, J. *J. Am. Chem. Soc.* **1996**, *118*, 12777.

(57) Maroulis, G. *J. Chem. Phys.* **1998**, *108*, 5432.

(58) Agmon, A. *Chem. Phys. Lett.* **1995**, *244*, 456; *J. Phys. Chem*. **1998**, *102*, 192.

(59) Impey, R. W.; Madden, P. A.; McDonald, I. R. *J. Phys. Chem.* **1983**, *87*, 5071.

(60) Copestake, A. P.; Neilson, G. W.; Enderby, J. E. *J. Phys. Solid State Phys.* **1985**, *18*, 4216.
(61) Blum, L.; Fawcett, W. R. *J. Phys. Chem.* **1992**, *96*, 408.
(62) Basilevsky, M. V.; Parsons, D. F. *J. Chem. Phys.* **1996**, *105*, 3734.
(63) Hewish, N. A.; Enderby, J. E.; Howells, W. S. *J. Phys. Solid State Phys.* **1983**, *16*, 1777.
(64) Petersen, C. P.; Gordon, M. S. *J. Phys. Chem. A* **1999**, *103*, 4162.
(65) Buchner, R.; Hefter, G. T.; May, P. M., *J. Phys. Chem. A* **1999**, *103*, 1.
(66) Marti, J.; Csajka, F. S. *J. Chem. Phys.* **2000**, *113*, 1154.
(67) Gauduel, Y.; Migus, A.; Chambaret, J. P.; Antonetti, A. *Rev. Phys. Appl.* **1987**, *22*, 1755. Gauduel, Y.; Pommeret, S.; Migus, A.; Yamada, N.; Antonetti, A. *J. Opt. Soc. Am. B* **1990**, *7*, 1528.
(68) Long, F. H.; Lu, H.; Eisenthal, K. B. *J. Chem. Phys.* **1989**, *91*, 4193. Long, F. H.; Shi, X.; Lu, H.; Eisenthal, K. B. *J. Phys. Chem.* **1994**, *98*, 7252.
(69) Gauduel, Y.; Pommeret, S.; Migus, A.; Yamada, N.; Antonetti, A. *J. Am. Chem. Soc*. **1990**, *112*, 2925.
(70) Yu, H.; Karplus, M. *J. Chem. Phys.* **1988**, *89*, 2366. Bader, S. J.; Chandler, D. *Chem. Phys. Lett.* **1989**, *157*, 501.
(71) Rossky, P. J. *J. Opt. Soc. Am.* **1990**, *B7*, 1727. Webster, F.; Rossky, P. J.; Friesner, R. A. *Comput. Phys. Com.* **1991**, *63*, 494. Webster, F.; Schnitker, J.; Friedrichs, M.; Friesner R. A.; Rossky P. J. *Phys. Rev. Lett*. **1991**, *66*, 3172. Webster, F.; Wang, E. T.; Rossky, P. J.; Friesner, R. A. *J. Chem. Phys*. **1994**, *100*, 4835. Prezhdo, O. V.; Rossky, P. J. *J. Chem. Phys.* **1997**, *107*, 5863. Yang, C. Y.; Wong, K. F.; Skaf, M. S.; Rossky, P. J. *J. Chem. Phys.* **2001**, *114*, 3598.
(72) Sprik, M.; Klein, M. L. *J. Chem. Phys*. **1988**, *89*, 7556. Laasonen, K.; Sprik, M.; Parrinello, M.; Car, R. *J. Chem. Phys*. **1993**, *99*, 9080. Tuckerman, M.; Laasonen, K.; Sprik, M.; Parrinello, M. *J. Phys. Chem*. **1995**, *99*, 5749; *J. Chem. Phys*. **1995**, *103*, 150.
(73) Clementi, E.; Corongiu, G.; Bahattacharya, D.; Feuston, B.; Frye, D.; Preiskorn, A.; Rizzo, A.; Xue, W. *Chem. Rev.* **1991**, *91*, 679.
(74) Barnett, R. B.; Landman, U.; Nitzan, A. *J. Chem. Phys.* **1989**, *90*, 4413; *J. Chem. Phys.* **1990**, *93*, 8187. Neria, E.; Nitzan, A.; Barnett, R. N.; Landman, U. *Phys. Rev. Lett.* **1991**, *67*, 1011. Makov, G.; Nitzan, A. *J. Phys. Chem.* **1994**, *98*, 3459.
(75) Pommeret, S.; Gauduel, Y. *J. Phys. Chem.* **1991**, *95*, 4126.
(76) Sheu, W. S.; Rossky, P. J. *Chem. Phys. Lett*. **1993**, *213*, 233. Schwartz, B. J.; Rossky P. J. *Phys. Rev. Lett*. **1994**, *72*, 3282; *J. Chem. Phys*. **1994**, *101*, 6902; *J. Chem. Phys*. **1994**, *101*, 6917; *J. Phys. Chem*. **1995**, *99*, 2953. Schwartz, B. J.; Rossky, P. J. *J. Chem. Phys*. **1996**, *105*, 6997; *J. Phys. Chem*. **1996**, *100*, 1295. Prezhdo, O. V.; Rossky, P. J. *J. Phys. Chem*. **1996**, *100*, 17094.
(77) Borgis, D.; Staib, A. *Chem. Phys. Lett*. **1994**, *230*, 405. Staib, A.; Borgis, D. *J. Chem. Phys.* **1995**, *103*, 2642.
(78) Chong, S. H.; Hirata, F. *J. Chem. Phys*. **1999**, *111*, 3654.
(79) Sprik, M. *J. Phys. Chem.* **1991**, *95*, 2283.
(80) Asada, T.; Nishimoto, K.; Kitaura, K., *J. Phys. Chem.* **1993**, *97*, 7724.
(81) Stuart, S.; Berne, B. J. *J. Phys. Chem.* **1996**, *100*, 11934.
(82) Matheson, M. S.; Mulac, W. A.; Rabani, J. *J. Phys. Chem*. **1963**, *67*, 2613.
(83) Jortner, J.; Ottolenghi, M.; Stein, G. *J. Phys. Chem.* **1964**, *68*, 247.
(84) Blandamer, M. J.; Fox, M. F. *Chem. Rev.* **1969**, *70*, 59.
(85) Shu, W. S.; Rossky, P. J. *J. Am. Chem. Soc.* **1993**, *115*, 7729.
(86) Markovich, G.; Pollack, S.; Giniger, R.; Cheshnovsky, O. *J. Chem. Phys.* **1994**, *101*, 9344. Serxner, D.; Dessent, C. E.; Jonhson, M. A. *J. Chem. Phys.* **1996**, *105*, 7231.
(87) (a) Gauduel, Y.; Gelabert, H.; Ashokkumar, M. *Chem. Phys*. **1995**, *197*, 167. (b) Gauduel, Y.; Gelabert, H.; Ashokkumar, M. *J. Mol. Liq*. **1995**, *64*, 57. (c) Gelabert, H.; Gauduel, Y. *J. Phys. Chem*. **1996**, *100*, 13993. (d) Gauduel, Y.; Sander, M.; Gelabert, H. *J. Chim. Phys*. **1996**, *93*, 1608.
(88) Kloepfer, J. A.; Vilchiz, V. H.; Lenchenkov, V. A.; Germaine, A. C.; Bradforth, S. E. *J. Chem. Phys.* **2000**, *113*, 6288. Bradforth, S.; Jungwirth, P. *J. Phys. Chem. A* **2002**, *106*, 1286.
(89) Barthel, E. R.; Martini, I. B.; Schwartz, B. J. *J. Phys. Chem. B* **2001**, *105*, 12230.
(90) Assel, M.; Laenen, R.; Laubereau, A. *Chem. Phys. Lett.* **1998**, *289*, 267.
(91) Staib, A.; Borgis, D. *J. Chem. Phys.* **1996**, *104*, 4776, 9027.
(92) Gauduel, Y.; Gelabert, H. *Chem. Phys*. **2000**, *256*, 333.
(93) Tazaki, K.; Doi, J. *J. Phys. Chem.* **1996**, *100*, 14520.
(94) Consta, S.; Kapral, R. *J. Chem. Phys.* **1999**, *111*, 10183.
(95) Chandra, A., *J. Chem. Phys. A* **1999**, *110*, 1569.
(96) Gauduel, Y.; Sander, M.; Gelabert, H. *J. Phys. Chem. A* **1998**, *102*, 7795.
(97) Gauduel, Y.; Gelabert, H.; Guilloud, F. *J. Am. Chem. Soc*. **2000**, *122*, 5082.
(98) (a) Wolff, R. K.; Bronskill, M. J.; Hunt, J. W. *J. Chem. Phys*. **1970**, *53*, 4211. (b) Wolff, R. K.; Aldrich, J. E.; Penner, T.; Hunt, J. W. *J. Phys. Chem*. **1975**, *79*, 210.
(99) Zapalowski, M.; Bartczak, W. *Res. Chem. Int*. **2001**, *27*, 855.
(100) Biakov, V. M.; Sharanin, Y. I.; Shubin, V. N. *Ber. Bunsen-Ges.* **1971**, *75*, 678.
(101) Brodsky, A. M.; Tsarevsky, A. V. *Chem. Phys*. **1980**, *44*, 483.
(102) Kreitus, I. *J. Phys. Chem*. **1985**, *89*, 1987.
(103) Czapski, G.; Peled, E. *J. Phys. Chem.* **1973**, *77*, 893.
(104) Lam, K. Y.; Hunt, J. W. *Int. Radiat. Phys. Chem*. **1975**, *7*, 317.
(105) Jonah, C. D.; Miller, J. R.; Hart, E. R.; Matheson, M. S. *J. Phys. Chem*. **1975**, *79*, 2705. Jonah, C. D.; Matheson, M. S.; Miller, J. R.; Hart E. J. *J. Phys. Chem*. **1976**, *80*, 1267. Jonah, C. D.; Miller, J. R.; Matheson, M. S. *J. Phys. Chem*. **1977**, *81*, 1618. Lewis, M. A.; Jonah, C. D. *J. Phys. Chem*. **1986**, *90*, 5367.
(106) Razem, D.; Hamill, W. H. *J. Phys. Chem*. **1977**, *81*, 1625.
(107) Bernal-Uruchurtu, M. I.; Ortega-Blake, I. *J. Chem. Phys.* **1995**, *103*, 1588.
(108) Carminiti, R.; Licheri, G.; Paschina, G.; Piccaluga, G.; Pinna, G. *Z. Naturforsch*. **1980**, *35a*, 1361.
(109) Bleuzen, A.; Foglia, F.; Furet, E.; Helm, L.; Merbach, A. E.; Weber, J. *J. Am. Chem. Soc*. **1996**, *118*, 12777 and references therein.
(110) Bopp, P. In The *Physical Chemistry of Aqueous Ionic Solutions*; Bellissent-Funel, M. C., Neilson, G. W., Eds.; Reidel: Dordrecht, The Netherlands, 1987; p 217.
(111) Sevilla, M. D.; Summerfield, S.; Eliezer, I.; Rak, J.; Symons, M. C. R. *J. Phys. Chem*. **1997**, *101*, 2910.
(112) Gauduel, Y.; Hallou, A. *Res. Chem. Intermed.* **2001**, *27*, 359.
(113) Kee, T. W.; Son, D. H.; Kambhampati, P.; Barbara, P. F. *J. Phys. Chem. A* **2001**, *105*, 8434.
(114) Deniz, A. A.; Li, B.; Peters, K. S. *J. Phys. Chem.* **1995**, *99*, 12209.
(115) Marcus, R. A. *J. Phys. Chem.* **1997**, *101*, 4072.